BTeV's Physics Goals, Sensitivities and Comparisons with Other Experiments

BTeV Collaboration

March 19, 2003

Contents

1.1 Introduction

In this document we answer the following question from P5: *Physics goals, including measurements to be made. For each measurement, what is the expected precision for measuring Standard Model Parameters and/or the expected sensitivity to new physics? How does this sensitivity compare to other existing or proposed experiments (for BTeV compare explicitly to what can be expected from the B-factories, CDF and D-Zero, as well as LHCb)? For each measurement, what are the uncertainties stemming from hadronic physics or other physics? Are there physics topics for which one of CDF or D-Zero will provide a significantly better measurement than the other detector?*

To answer this question we will discuss the physics of BTeV. We will define the Standard Model parameters and provide our estimates of the errors obtainable with BTeV. Our extremely good sensitivity to New Physics can be viewed in terms of generic tests or in the context of specific models. Since it is much easier to quantify this sensitivity in the context of specific models we will do that. Comparisons with other experiments will be documented near the end.

We know that the Standard Model cannot explain the baryon asymmetry of the Universe and problem of extra matter in galaxies, called "Dark Matter." Therefore, there is New Physics out there that we need to find. There are many other reasons why we believe that the Standard Model is incomplete and there must be physics beyond. One is the plethora of "fundamental parameters," for example quark masses, mixing angles, etc... The Standard Model cannot explain the smallness of the weak scale compared to the GUT or Planck scales; this is often called "the hierarchy problem." It is believed that the CKM source of CP violation in the Standard Model is not large enough to explain the baryon asymmetry of the Universe [1]; thus it is very possible that there are large yet unknown CP violation sources that we will discover in b and/or c decays. Finally, gravity is not incorporated. John Ellis said "My personal interest in CP violation is driven by the search for physics beyond the Standard Model" [2]. (A more complete description of the basic physics is given in Chapter 1 of our 2002 Proposal Update http://www-btev.fnal.gov/cgi-bin/public/DocDB/ShowDocument?docid=316 .)

BTeV has many physics goals. The major branches include finding new physics or refining our understanding of new physics found elsewhere, e.g. the LHC, using both CP violating phases and rare b and c decays. It is also important to precisely measure Standard Model parameters. Other physics goals include studies of QCD in weak decay processes probed by measuring branching ratios, semileptonic form- factors, polarizations in vector-vector decays and Dalitz plots in three-body decays, b and c quark production, structure of b states including baryon decays and B_c decays. We fully expect that more than 100 Ph. D. theses will be written on BTeV data.

1.2 The CKM Matrix and the CKM Angles

The gauge bosons, $W^{\pm}$, γ and Z^o couple to mixtures of the physical d, s and b states. This mixing is described by the Cabibbo-Kobayashi-Maskawa (CKM) matrix [3]. In the Wolfenstein approximation the matrix is written in order λ^3 for the real part and λ^4 for the imaginary part as [4]

$$V_{CKM} = \begin{pmatrix} 1-\lambda^2/2 & \lambda & A\lambda^3(\rho - i\eta)(1-\lambda^2/2) \\ -\lambda & 1-\lambda^2/2 - i\eta A^2\lambda^4 & A\lambda^2(1+i\eta\lambda^2) \\ A\lambda^3(1-\rho-i\eta) & -A\lambda^2 & 1 \end{pmatrix}. \qquad (1.1)$$

The parameters λ, A, ρ and η, are fundamental constants of nature, just as basic as G, Newton's constant, or α_{EM}. Two are determined from charged-current weak decays. The measured values are $\lambda = 0.2205 \pm 0.0018$ and A=0.784±0.043. There are constraints on ρ and η from other measurements. (Usually the matrix is viewed only up to order λ^3. To explain CP violation in the K^o system the term of order λ^4 in V_{cs} is necessary.)

The unitarity of the CKM matrix allows us to construct six relationships. These may be thought of as triangles in the complex plane shown in Fig. 1.1.

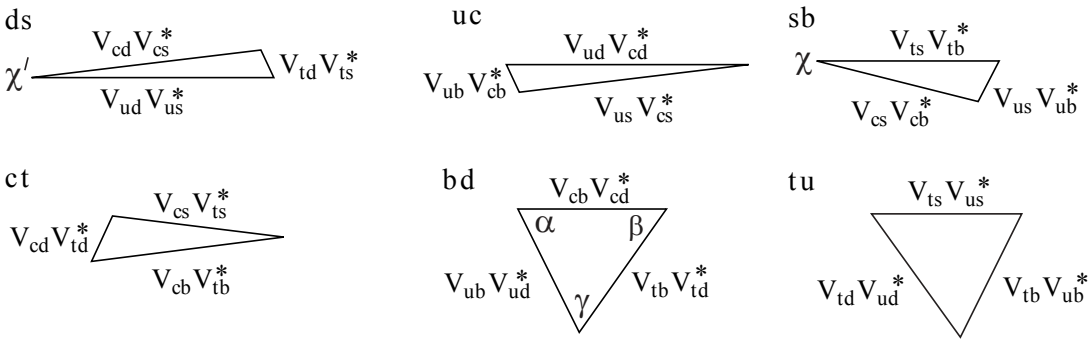

Figure 1.1: The six CKM triangles. The bold labels, e.g. **ds** refer to the rows or columns used in the unitarity relationship. The angles defined in equation (1.2) are also shown.

All six of these triangles can be constructed knowing four and only four independent angles [5][6][7]. These are defined as:

$$\beta = arg\left(-\frac{V_{tb}V_{td}^*}{V_{cb}V_{cd}^*}\right), \qquad \gamma = arg\left(-\frac{V_{ub}^*V_{ud}}{V_{cb}^*V_{cd}}\right), \qquad (1.2)$$

$$\chi = arg\left(-\frac{V_{cs}^*V_{cb}}{V_{ts}^*V_{tb}}\right), \qquad \chi' = arg\left(-\frac{V_{ud}^*V_{us}}{V_{cd}^*V_{cs}}\right). \qquad (1.3)$$

(α can be used instead of γ or β.) Two of the phases β and γ are probably large while χ is estimated to be small ≈0.02, but measurable, and χ' is likely to be much smaller.

The current situation is summarized by Nir [8] (see Fig. 1.2). Here the value $\sin(2\beta)$ is compared on the $\rho - \eta$ plane with a fit to measurements of $|V_{ub}|$ and $|V_{cb}|$, ϵ_K, from CP violation in K_L decay, B_d mixing and an upper limit on the ratio of B_s to B_d mixing. In all measurements but $\sin(2\beta)$, the theoretical errors in deriving constraints on ρ and η from the measurements are dominant.

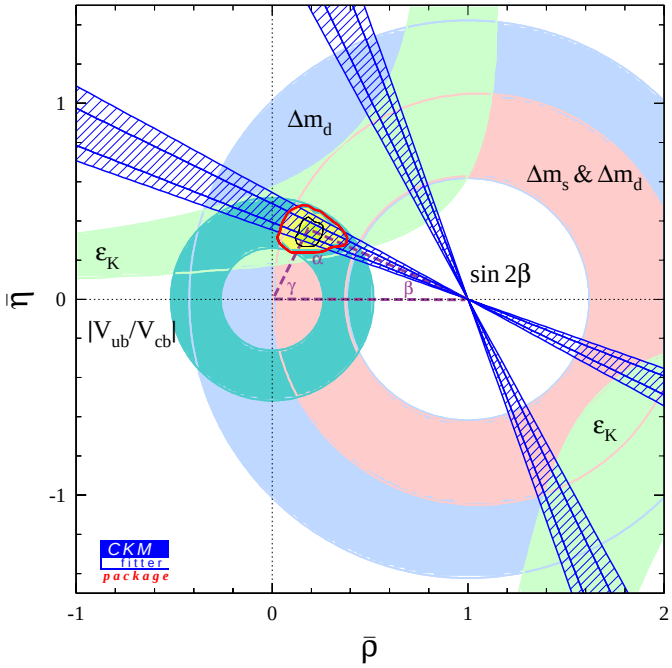

Figure 1.2: Fits in the $\rho - \eta$ plane using data from CP violation in K^o decay (ϵ_K), $|V_{ub}/V_{cb}|$ and the ratio of B_s mixing (Δm_s) to B_d mixing (Δm_d) compared with the measurement of $\sin(2\beta)$ from the Babar and Belle collaborations. The angles α, γ and one possibility for β are also indicated. ($\overline{\rho} = \rho(1 - \lambda^2/2$, with a similar definition for $\overline{\eta}$.) From Nir [8].

In performing the fit, the theory parameters are allowed to have equal probability within a restricted but arbitrary range [9]. Therefore, there is a large model dependence for parameter space restricted by measurements of (ϵ_K), $|V_{ub}/V_{cb}|$ and Δm_d, with a smaller but significant model dependence for $\Delta m_s/\Delta m_d$. The data are surely consistent although the 4-fold ambiguity in β, due to the fact that we measure $\sin(2\beta)$, does allow for a rather large surprise.

1.3 Testing for and Defining New Physics

1.3.1 Generic Tests

We can look for New Physics either in the context of specific models or more generically, for deviations from the Standard Model expectation independent of specific non-standard models. This can be done for both CP violating decays and rare decays. Let us start with generic tests using CP violation.

1.3.1.1 A Critical Check Using χ

It has been pointed out by Silva and Wolfenstein [5] that measuring only angles may not be sufficient to detect new physics. For example, suppose there is new physics that arises in $B^o - \overline{B}^o$ mixing. Let us assign a phase θ to this new physics. If we then measure CP violation in $B^o \to J/\psi K_s$ and $B^o \to \rho\pi$, then we actually measure $2\beta' = 2\beta + \theta$ and $2\alpha' = 2\alpha - \theta$. So while there is new physics, we miss it, because $2\beta' + 2\alpha' = 2\alpha + 2\beta$ and $\alpha' + \beta' + \gamma = 180°$.

Measurements of the magnitudes of CKM matrix elements, however, all come with theoretical errors. Some of these are hard to estimate. The best measured magnitude is that of $\lambda = |V_{us}/V_{ud}| = 0.2205 \pm 0.0018$. Silva and Wolfenstein [5] [6] show that the Standard Model can be checked in a profound manner by seeing if:

$$\sin\chi = \left|\frac{V_{us}}{V_{ud}}\right|^2 \frac{\sin\beta\ \sin\gamma}{\sin(\beta+\gamma)} \quad . \tag{1.4}$$

Here the precision of the check will be limited initially by the measurement of $\sin\chi$, not of λ. (BTeV can measure χ using the reaction $B_s \to J\psi\eta^{(\prime)}$.) This check can reveal new physics, even if other measurements have not shown any anomalies.

1.3.1.2 Finding Inconsistencies

Another interesting way of viewing the physics was given by Peskin [10], and illustrated in Fig. 1.3. Non-Standard Model physics would show up as discrepancies among the values of (ρ, η) derived from independent determinations using CKM magnitudes ($|V_{ub}/V_{cb}|$ and $|V_{td}/V_{ts}|$), or B_d^o mixing (β and α), or B_s mixing (χ and γ).

1.3.1.3 Generic Tests for New Physics Using Rare Decays

The basic structure of "Rare b Decays," is shown by the loop diagram shown in Fig. 1.4. Here a photon, dilepton pair or gluon can be radiated off any charged particle leg. In the case of the $\ell^+\ell^-$ pair there can be an intermediate photon or Z^o. New charged objects can replace quarks and new gauge-like objects can replace the W^-. Since calculations where the gluon is radiated are more difficult, we will focus mainly on the electromagnetic decays. We consider both inclusive decays such as $b \to s\gamma$, $b \to d\gamma$ and $b \to s\ell^+\ell^-$ and their exclusive counterpoints, $B \to K^*\gamma$, $B \to \rho\gamma$ and $B \to K^*\ell^+\ell^-$.

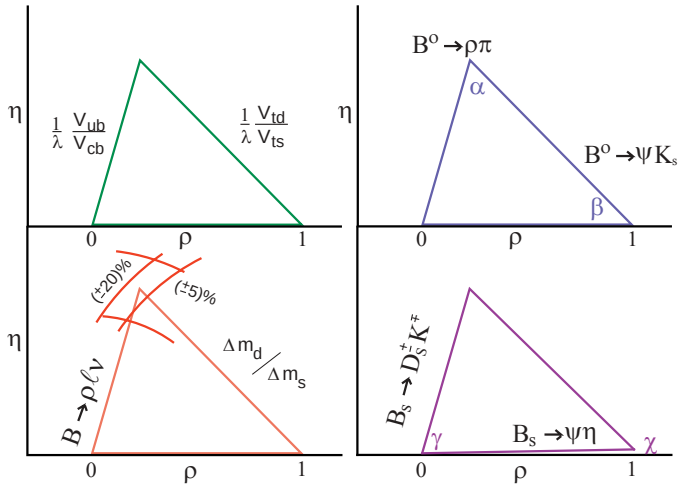

Figure 1.3: One of the CKM triangles showing how it is possible to find the values of η and ρ using three sets of independent measurements based on CP violating decays going via B^o mixing (upper right), CP violating decays going via B_s mixing (lower right), or magnitudes of CKM elements (upper left), with some estimate of the ultimate theoretical errors (lower left). Adopted from Peskin [10].

Greub, Ioannissian and Wyler [11] write: ".. the decay into $B \to K^* \ell^+ \ell^-$ yields a wealth of new information on the form of the new interactions since the Dalitz plot is sensitive to subtle interference effects."

1.3.2 New Physics Tests in Specific Models

1.3.2.1 Supersymmetry

Supersymmetry is a set of many models. The basic idea is that for every fundamental fermion there is a companion boson and for every boson there is a companion fermion. There are many different implementations of couplings in this framework [12]. In the most general case

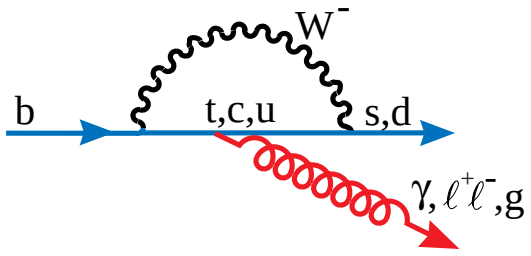

Figure 1.4: Quark level diagram for second order weak processes, often called "penguins" in the literature.

we pick up 80 new amplitudes and 43 new phases. This is clearly too many to handle so we can try to see things in terms of simpler implementations. In the minimum model (MSSM) we have only two new fundamental phases. One, θ_D, would arise in B^o mixing and the other, θ_A, would appear in B^o decay. A combination would generate CP violation in D^o mixing, call it $\phi_{K\pi}$ when the $D^o \to K^-\pi^+$ [13]. Table 1.1 shows the CP asymmetry in three different processes in the Standard Model and the MSSM.

Table 1.1: CP Violating Asymmetries in the Standard Model and the MSSM.

Process	Standard Model	New Physics
$B^o \to J/\psi K_s$	$\sin 2\beta$	$\sin 2(\beta + \theta_D)$
$B^o \to \phi K_s$	$\sin 2\beta$	$\sin 2(\beta + \theta_D + \theta_A)$
$D^o \to K^-\pi^+$	0	$\sim \sin \phi_{K\pi}$

Two direct effects of New Physics are clear here. First of all, the difference in CP asymmetries between $B^o \to J/\psi K_s$ and $B^o \to \phi K_s$ would show the phase ϕ_A. Secondly, there would be finite CP violation in $D^o \to K^-\pi^+$ where none is expected in the Standard Model.

Manifestations of specific SUSY models lead to different patterns. Table 1.2 shows the expectations for some of these models in terms of these variables and the neutron electric dipole moment d_N; see [13] for details. Note, that "Approximate CP" has already been ruled

Table 1.2: Some SUSY Predictions.

Model	$d_N \times 10^{-25}$	θ_D	θ_A	$\sin \phi_{K\pi}$
Standard Model	$\leq 10^{-6}$	0	0	0
Approx. Universality	$\geq 10^{-2}$	$\mathcal{O}(0.2)$	$\mathcal{O}(1)$	0
Alignment	$\geq 10^{-3}$	$\mathcal{O}(0.2)$	$\mathcal{O}(1)$	$\mathcal{O}(1)$
Heavy squarks	$\sim 10^{-1}$	$\mathcal{O}(1)$	$\mathcal{O}(1)$	$\mathcal{O}(10^{-2})$
Approx. CP	$\sim 10^{-1}$	$-\beta$	0	$\mathcal{O}(10^{-3})$

out by the measurements of $\sin 2\beta$.

Using the MSSM model, Hinchcliff and Kersting predict there will be significant contributions to B_s mixing, and the CP asymmetry in the charged decay $B^\mp \to \phi K^\mp$ [14]. The contribution to B_s mixing significantly enhances the CP violating asymmetry in modes such as $B_s \to J/\psi\eta$. (Recall the CP asymmetry in this mode is proportional to $\sin 2\chi$ in the Standard Model.) The Standard Model diagram and MSSM diagrams are shown in Fig. 1.5. The expected CP asymmetry in the MSSM is $\approx \sin\phi_\mu \cos\phi_A \sin(\Delta m_s t)$, which is approximately 10 times the expected value in the Standard Model.

We observed that a difference between CP asymmetries in $B^o \to J/\psi K_s$ and ϕK_s arises in the MSSM due to a CP asymmetry in the decay phase. It is possible to observe this

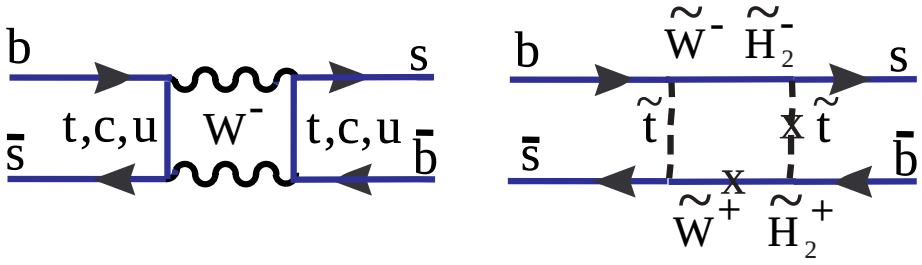

Figure 1.5: The Standard Model (left) and MSSM (right) contributions to B_s^o mixing.

directly by looking for a CP asymmetry in $B^{\mp} \to \phi K^{\mp}$. The Standard Model and MSSM diagrams are shown in Fig. 1.6. Here the interference of the two diagrams provides the CP asymmetry. The predicted asymmetry is equal to $\left(M_W/m_{squark}\right)^2 \sin\phi_\mu$ in the MSSM, where m_{squark} is the relevant squark mass [14].

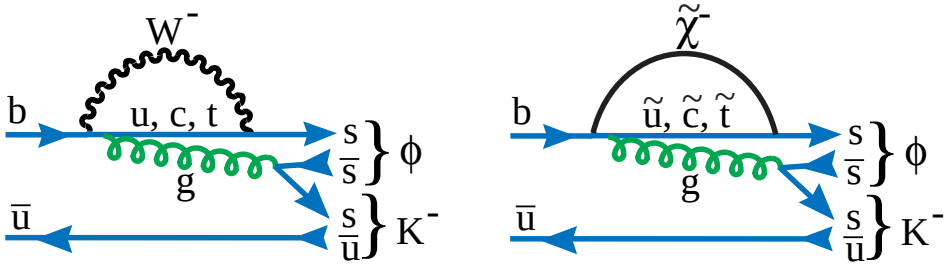

Figure 1.6: The Standard Model (left) and MSSM (right) contributions to $B^- \to \phi K^-$.

The ϕK and ϕK^* final states have been observed, first by CLEO [15] and subsequently by BABAR [16]. The average branching ratio is $\mathcal{B}(B^- \to \phi K^-) = (6.8 \pm 1.3) \times 10^{-6}$ showing that in principle large samples can be acquired especially at hadronic machines.

The polarization in the rare decay $B \to K^* \ell^+ \ell^-$ is also a very effective way of sorting out supersymmetric models. Fig. 1.7 shows the predicted forward-backward polarization as a function of s, the dilepton invariant mass squared, from Ali *et al.*, [17] for the Standard Model and a collection of supersymmetric models.

In a different work, Ali *et al.* tell us: "Precise measurements of the dilepton invariant mass distributions in the decays $B \to (s, K^*)\ell^+\ell^-$ will greatly help in discriminating among the Standard Model and various supersymmetric theories" [18].

1.3.2.2 Extra Dimensions

Papers predicting changes in B decay phenomena when the world has extra physical dimensions are listed in ref. [19]. Another paper by Aranda *et al.* relates quark and neutrino mixing in extra dimensions [20].

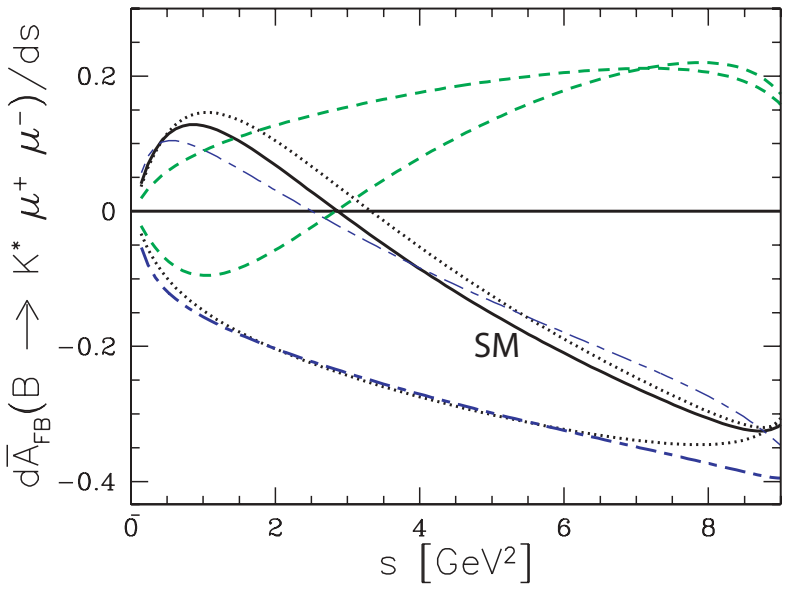

Figure 1.7: The normalized forward-backward asymmetry in $B \to K^* \mu^+ \mu^-$ decay as a function of s, the dilepton invariant mass squared using the form factors from the LCSR approach. The solid line denotes the SM prediction. The dotted (long-short dashed) lines correspond to the SUGRA (the MIA-SUSY) model for different The dashed curves indicating a positive asymmetry for large s correspond to the MIA-SUSY models for the "best depression scenario." (From ref. [17]).

Buras *et al.* [21] have considered a model of one universal extra dimension compactified at a scale of $1/R > 250$ GeV, based on the work of Appelquist, Cheng and Dobrescu (ACD) [22]. The contributions from the Kaluza-Klein modes produce no effect on the major components now used to determine ρ and η, namely, $|V_{ub}/V_{cb}|$, $\Delta m_s/\Delta m_d$ and $\sin(2\beta)$. However, there are significant effects on the value of V_{td}, the size of γ and branching ratio for $B^o \to \mu^+\mu^-$ as shown in Fig. 1.8

More precise measurements are required to differentiate between the Standard Model and this model as $1/R$ increases.

1.3.2.3 SO(10)

A strong connection is made between neutrino mixing and CP violation in the quark sector in a paper by Chang, Masiero and Murayama [23]. In this model the large mixing between ν_μ and ν_τ (from atmospheric neutrino oscillations) can lead to large mixing between b_R and s_R. This does not violate any known measurements and leads to large CP violation in B_s mixing, deviations from $\sin(2\beta)$ in the reaction $B^o \to \phi K_s$ and changes in the phase γ.

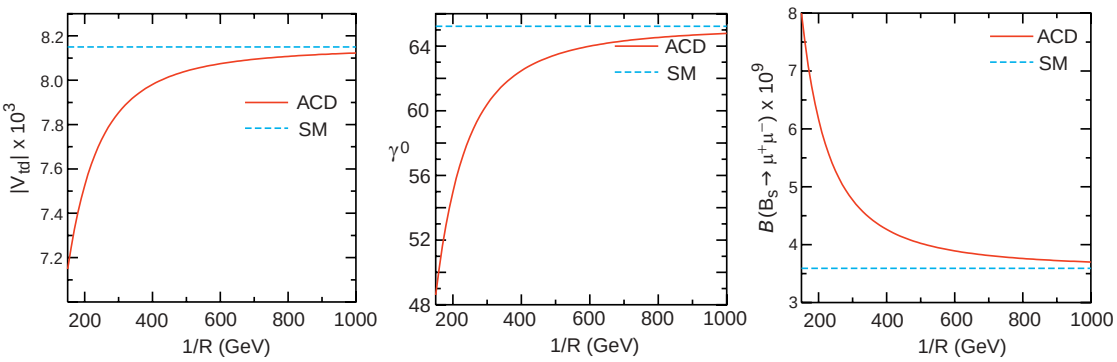

Figure 1.8: The effect on measured quantities of one extra dimension (ACD) compared with the Standard Model (SM) as a function of the compactification scale R.

1.3.2.4 Other New Physics Models

There are many other specific models that predict New Physics in b decays. we list here a few of these with a woefully incomplete list of references, to give a flavor of what these models predict.

- *Two Higgs and Multi-Higgs Doublet Models-* They predict large effects in ϵ_K and CP violation in $D^o \to K^-\pi^+$ with only a few percent effect in B^o [13]. Expect to see 1-10% CP violating effects in $b \to s\gamma$ [24].

- *Left-Right Symmetric Model-* Contributions compete with or even dominate over Standard Model contributions to B_d and B_s mxing. This means that CP asymmetries into CP eigenstates could be substantially different from the Standard Model prediction [13].

- *Extra Down Singlet Quarks-* Dramatic deviations from Standard Model predictions for CP asymmetries in b decays are not unlikely [13].

- *FCNC Couplings of the Z boson-* Both the sign and magnitude of the decay leptons in $B \to K^*\ell^+\ell^-$ carry sensitive information on new physics. Potential effects are on the of 10% compared to an entirely negligable Standard Model asymmetry of $\sim 10^{-3}$ [25].

- *Noncommutative Geometry-* If the geometry of space time is noncommutative, i.e. $[x_\mu, x_\nu] = i\theta_{\mu\nu}$, then CP violating effects may be manifest at low energy. For a scale <2 TeV there are comparable effects to the Standard Model [26].

- *MSSM without new flavor structure-* Can lead to CP violation in $b \to s\gamma$ of up to 5% [27]. Ali and London propose [28] that the Standard Model formulas are modified by Supersymmetry as

$$\Delta m_d \;=\; \Delta m_d(\mathrm{SM}) \left[1 + f\left(m_{\chi_2^\pm}, m_{\tilde{t}_R}, m_{H^\pm}, tan\beta\right)\right] \tag{1.5}$$

$$\Delta m_s = \Delta m_s(\mathrm{SM}) \left[1 + f\left(m_{\chi_2^\pm}, m_{\tilde{t}_R}, m_{H^\pm}, tan\beta\right)\right] \quad (1.6)$$

$$|\epsilon_K| = \frac{G_F^2 f_K^2 M_K M_W^2}{6\sqrt{2}\pi^2 \Delta M_K} B_K (A^2\lambda^6\overline{\eta}) \Big[y_c\left(\eta_{ct} f_3(y_c, y_t) - \eta_{cc}\right) + \eta_{tt} y_t f_s(y_t)\left[1 + f\left(m_{\chi_2^\pm}, m_{\tilde{t}_R}, m_{H^\pm}, tan\beta\right)\right] A^2\lambda^4(1-\overline{\rho})\Big] \quad , \quad (1.7)$$

where $\Delta m(SM)$ refers to the Standard Model formula and the expression for $|\epsilon_K|$ would be the Standard Model expression if f were set equal to zero. Ali and London show that it is reasonable to expect that $0.8 > f > 0.2$. Since the CP violating angles will not change from the Standard Model, determining the value of $(\rho,\ \eta)$ using the magnitudes $\Delta m_s/\Delta m_d$ and $|\epsilon_K|$ will show an inconsistency with values obtained using other magnitudes and angles.

1.3.3 Required Measurements Involving β

Besides a more precise measurement of $\sin 2\beta$ we need to resolve the four ambiguities. There are two suggestions on how this may be accomplished. Kayser [29] shows that time dependent measurements of the final state $J/\psi K^o$, where $K^o \to \pi\ell\nu$, give a direct measurement of $\cos(2\beta)$ and can also be used for CPT tests. Another suggestion is to use the final state $J/\psi K^{*o}$, $K^{*o} \to K_S\pi^o$, and to compare with $B_s \to J/\psi\phi$ to extract the sign of the strong interaction phase shift assuming SU(3) symmetry, and thus determine $\cos(2\beta)$ [30].

1.3.4 Required Measurements Involving α

It is well known that $\sin(2\beta)$ can be measured without problems caused by Penguin processes using the reaction $B^o \to J/\psi K_s$. The simplest reaction that can be used to measure $\sin(2\alpha)$ is $B^o \to \pi^+\pi^-$. This reaction can proceed via both the Tree and Penguin diagrams shown in Fig. 1.9.

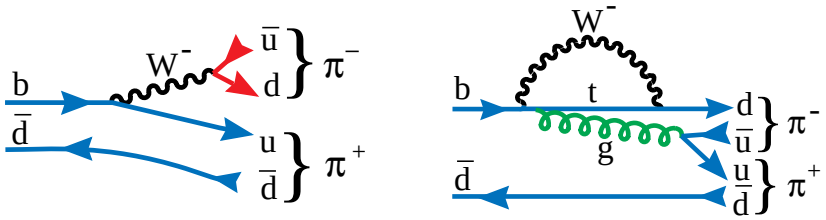

Figure 1.9: Decay diagrams for $\overline{B}^o \to \pi^+\pi^-$. (left) Via tree level V_{ub} moderated decay. (right) Via a Penguin process.

Current measurements show a large Penguin component. The ratio of Penguin *amplitude* to Tree *amplitude* in the $\pi^+\pi^-$ channel is about 40% in magnitude. Thus the effect of the Penguin must be determined in order to extract α. The only model independent way of doing

this was suggested by Gronau and London, but requires the measurement of $B^{\mp} \to \pi^{\mp}\pi^{o}$ and $B^{o} \to \pi^{o}\pi^{o}$, the latter being rather daunting.

There is, however, a theoretically clean method to determine α. The interference between Tree and Penguin diagrams can be exploited by measuring the time dependent CP violating effects in the decays $B^{o} \to \rho\pi \to \pi^{+}\pi^{-}\pi^{o}$ as shown by Snyder and Quinn [31].

The $\rho\pi$ final state has many advantages. These final states were first seen by CLEO with large rates relative to $\pi\pi$. Table 1.3 lists the current measurements.

Table 1.3: Measurements of $B \to \rho\pi$ Branching Ratios ($\times 10^{-6}$) or upper limits at 90% confidence level.

Reaction	CLEO [32]	BABAR [33]	BELLE [34]	Average
$B^{-} \to \rho^{o}\pi^{-}$	$10.4^{+3.3}_{-3.4} \pm 2.1$	-	$8.0^{+2.3+0.7}_{-2.0-0.7}$	8.6±2.0
$B^{o} \to \rho^{\pm}\pi^{\mp}$	$27.6^{+8.4}_{-7.4} \pm 4.2$	$28.9 \pm 5.4 \pm 4.3$	$20.8^{+6.0+2.8}_{-6.3-3.1}$	25.4±4.3
$B^{o} \to \rho^{o}\pi^{o}$	<5.5	-	<5.3	-

These measurements are consistent with some theoretical expectations [35]. Furthermore, the associated vector-pseudoscalar Penguin decay modes have conquerable or smaller branching ratios. Secondly, since the ρ is spin-1, the π spin-0 and the initial B also spinless, the ρ is fully polarized in the (1,0) configuration, so it decays as $\cos^2\theta$, where θ is the angle of one of the ρ decay products with the other π in the ρ rest frame. This causes the periphery of the Dalitz plot to be heavily populated, especially the corners. A sample Dalitz plot is shown in Fig. 1.10. This kind of distribution is good for maximizing the interferences, which helps minimize the error. Furthermore, little information is lost by excluding the Dalitz plot interior, a good way to reduce backgrounds.

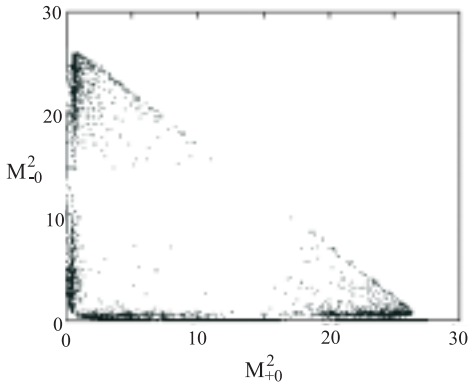

Figure 1.10: The Dalitz plot for $B^{o} \to \rho\pi \to \pi^{+}\pi^{-}\pi^{o}$ from Snyder and Quinn.

To estimate the required number of events Snyder and Quinn preformed an idealized analysis that showed that a background-free, flavor-tagged sample of 1000 to 2000 events was sufficient. The 1000 event sample usually yields good results for α, but sometimes does not resolve the ambiguity. With the 2000 event sample, however, they always succeeded.

This technique not only finds $\sin(2\alpha)$, it also determines $\cos(2\alpha)$, thereby removing two of the remaining ambiguities. The final ambiguity can be removed using the CP asymmetry in $B^o \to \pi^+\pi^-$ and a theoretical assumption [36].

1.3.5 Required Measurements Involving γ

It may be easier to measure γ than α in a model independent manner. There have been two methods suggested.

(1) Time dependent flavor tagged analysis of $B_s \to D_s^{\pm}K^{\mp}$. This is a direct model independent measurement [37]. Here the Cabibbo suppressed V_{ub} decay interferes with a somewhat less suppressed V_{cb} decay via B_s mixing as illustrated in Fig. 1.11 (left). Even though we are not dealing with CP eigenstates here there are no hadronic uncertainties, though there are ambiguities. Since this proceeds via B_s mixing the exact CP violating angle measured is $\gamma - 2\chi$.

(2) Measure the rate differences between $B^- \to \overline{D}^o K^-$ and $B^+ \to D^o K^+$ in two different D^o decay modes such as $K^-\pi^+$ and K^+K^-. This method makes use of the interference between the tree and doubly-Cabibbo suppressed decays of the D^o, and does not depend on any theoretical modeling [38][39]. See Fig. 1.11 (right).

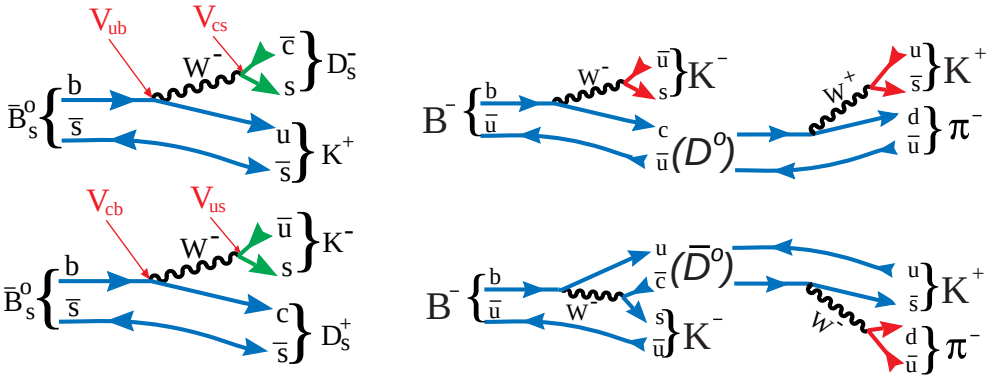

Figure 1.11: (left) The two diagram diagrams for $B_s \to D_s^{\pm}K^{\mp}$ that interfere via B_s mixing. (right) The two interfering decay diagrams for $B^- \to \overline{D}^o K^-$ where one is a $b \to u$ transition and the other a doubly-Cabibbo suppressed decay.

Several model dependent methods using the light two-body pseudoscalar decay rates have been suggested for measuring γ. The basic idea in all these methods can be summarized as follows: $B^o \to \pi^+\pi^-$ has the weak decay phase γ. In order to reproduce the observed suppression of the decay rate for $\pi^+\pi^-$ relative to $K^{\pm}\pi^{\mp}$ we require a large negative interference between the Tree and Penguin amplitudes. This puts γ in the range of 90°. There is a great deal of theoretical work required to understand rescattering, form-factors etc... We are left with several ways of obtaining model dependent limits, due to Fleischer and Mannel [40], Neubert and Rosner [41], Fleischer and Buras [42], and Beneke *et al.* [43]. The latter make a sophisiticated model of QCD factorization and apply corrections. These ideas may

be very useful for resolving ambiguities, but the amount of model dependence will remain a concern.

Another method for determining γ proposed by Fleischer [44] uses the assumption of U-spin symmetry ($d \Longleftrightarrow s$) and requires the measurement of both $B^o \to \pi^+\pi^-$ and $B_s \to K^+K^-$ CP asymmetries. Again the model dependence here is a concern, but it may be quite useful for ambiguity resolution.

1.3.6 Required Measurements Involving χ

The angle χ, defined in equation 1.2, can be extracted by measuring the time dependent CP violating asymmetry in the reaction $B_s \to J/\psi\eta^{(\prime)}$, or if one's detector is incapable of quality photon detection, the $J/\psi\phi$ final state can be used. However, in this case there are two vector particles in the final state, making this a state of mixed CP, requiring a time-dependent angular analysis to extract χ, that requires large statistics. Fig. 1.12 shows the decay diagram.

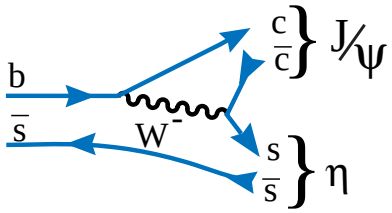

Figure 1.12: The decay diagram for $B_s \to J/\psi\eta$. The final state is a CP eigenstate.

Once χ, β and α or γ are precisely measured, then all the magnitudes of the CKM elements can be determined. The only model dependent theoretical error arises from the determination of λ, of the order of 1% [6].

1.3.7 Conclusions on Importance of b and c Decays

It is clear that precision studies of CP violating B_s, B^o and D^o decays, and rare decays, can bring a wealth of information to bear on new physics, that probably will be crucial in sorting out anything seen at the LHC. A picture of the effects on b physics by Hiller is illustrative and shown in Fig. 1.13 [45].

The connections of our physics studies with other experiments in the LHC era sketched in Fig. 1.14. Our studies of CP violation and rare decays will play a central role in sorting out new physics and providing clues to the flavor puzzle along with neutrino physics.

We close this section with a quote from Masiero and Vives [46]: "The relevance of SUSY searches in rare processes is not confined to the usually quoted possibility that indirect searches can arrive 'first' in signaling the presence of SUSY. Even after the possible direct observation of SUSY particles, the importance of FCNC and CP violation in testing SUSY

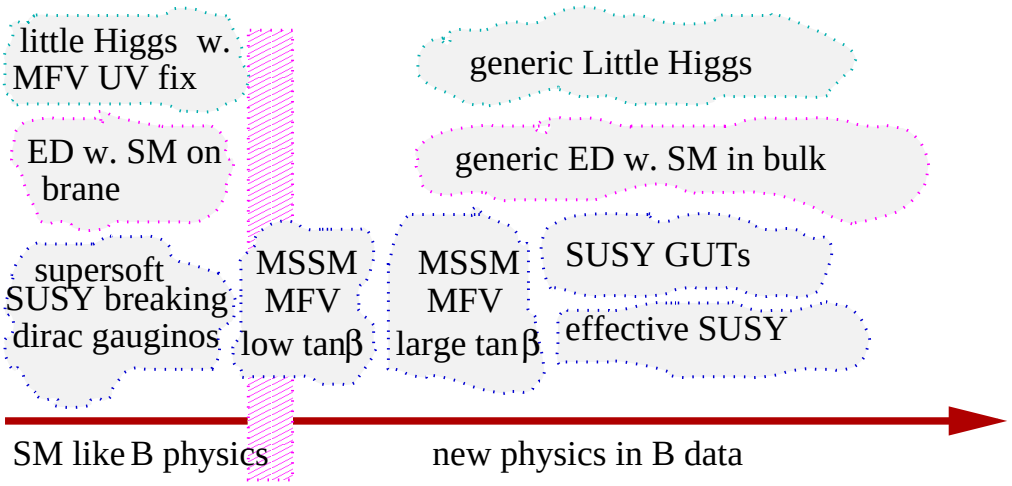

Figure 1.13: Effects on rare or CP violating B decays from different models of Electroweak symmetry breaking. (From Hiller [45].)

remains of utmost relevance. They are and will be complementary to the Tevatron and LHC establishing low energy supersymmetry as the response to the electroweak breaking puzzle."

We agree, except that we would replace "SUSY" with "New Physics."

1.4 BTeV's Physics Reach

We will now show that BTeV is well equipped to address all of the issues discussed above. BTeV can also investigate many other physics topics that we have not mentioned that may turn out to be of great import in the future, for example CPT violation [47].

The results quoted here are based on the tools described and studies reported in Part III, "Physics Simulations" of the May, 2000 BTeV proposal [48]. These studies were rigorous and extensive. In most case GEANT3 was used, where both signal events and background samples $\sim 10^7$ events were generated and reconstructed. These simulation results reflect those presented in our 2002 Proposal Update, for the most part, although there have been some additions and corrections due to further analysis.

1.4.1 Summary of Flavor Tagging

A detailed study of flavor tagging is given in the 2002 Proposal Update in section 2.10 (page 20 of Chapter 2). There we showed that we can achieve an effective flavor tagging efficiency, characterized as the product of the efficiency ϵ and the dilution D as ϵD^2 of 10% for B^o decays. This study also shows that, as expected, B_s decays have higher tagging efficiency because of the charged kaon produced to conserve flavor in the b quark fragmentation to a B_s. This "same side" tagging is quite favorable and, as a result, we achieve 13% for ϵD^2 in B_s decays.

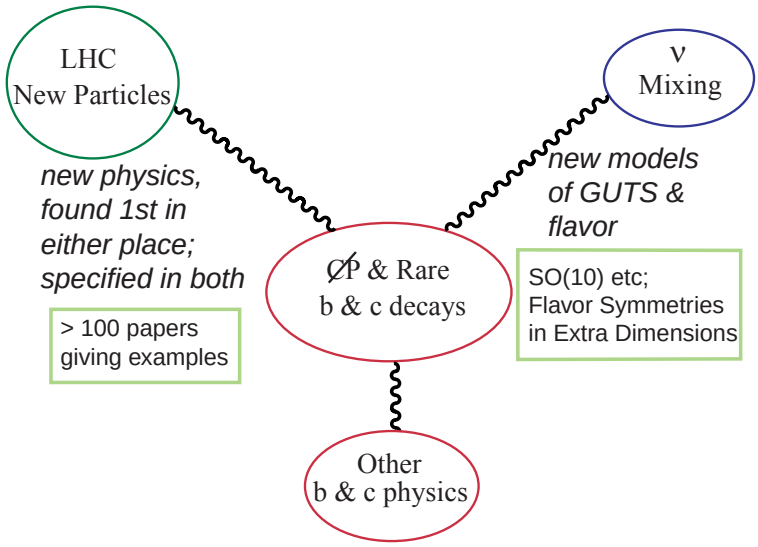

Figure 1.14: Links between studies of CP violation in b and c decays with searches for new phenomena at the LHC and experiments in the neutrino sector.)

1.4.2 Sensitivities to CP Violating Angles

BTeV will have outstanding performance in determining CP violating asymmetries. The results of our simulations are summarized in Table 1.4 for a luminosity of 2×10^{32} cm^{-2}s^{-1} and 10^7 seconds of running time. Descriptions of the analysis techniques used to obtain the signal and background yields are given in the BTeV Proposal.

All of the measurements listed here to determine χ, α, β, γ and x_s, except for the determination of γ using the $B \to K\pi$ modes, are completely free of hadronic uncertainties or errors due to theoretical models. Ultimately, at the level of errors below 1° for α, β and γ (and a much lower number for χ), the effects of other diagrams or higher order terms in the Wolfenstein approximation need to be considered. We are now far from this level of concern.

There are other ways to determine some of these angles that we have not discussed. Omission from this table, does not necessarily imply that we cannot use a particular technique, but merely that we have not yet simulated or completely considered the implications of that method. For example, measuring the CP asymmetry in the decay $B^o \to D^{*+}\pi^-$ has been shown to be a model independent way of measuring $(-2\beta - \gamma)$ [49]. On the other hand, the physical asymmetry is expected to be below 1%, making systematic errors in the efficiencies of detecting positive versus negative tracks, particularly the pion from the D^{*+} decay, a key issue. We simply have not yet evaluated this tantalizing approach.

We briefly discuss some of these measurements:

- We use the method proposed by Snyder and Quinn to determine α using $B^o \to \rho\pi \to \pi^+\pi^-\pi^o$ [50]. Both the signal efficiencies and the background levels were determined by a full GEANT simulation. We give details on our study that estimated the error in α below. Quinn and Silva have proposed using non-flavor-tagged rates as input to

Table 1.4: Yearly sensitivities to CP violating angles and related quantities. (Reactions between lines are used together.)

Reaction	$\mathcal{B} \times 10^{-6}$	# of Events	S/B	Parameter	Error (Value)
$B_s \to D_s^+ K^-$	300	7,500	7	$\gamma - 2\chi$	8°
$B_s \to D_s^+ \pi^-$	3000	59,000	3	x_s	(75)
$B^o \to J/\psi K_s$	445	168,000	10	$\sin(2\beta)$	0.017
$B^o \to J/\psi K^o$					
$K^o \to \pi^\pm \ell^\mp \nu$	7	250	2.3	$\cos(2\beta)$	$\sim$0.5
$B^o \to \pi^+ \pi^-$	4.5	14,600	3	Asymmetry	0.030
$B_s \to K^+ K^-$	17	18,900	6.6	Asymmetry†	0.020
$B^- \to \overline{D}^o (K^+\pi^-) K^-$	0.17	170	1		
$B^- \to \overline{D}^o (K^+K^-) K^-$	1.1	1000	>10	γ	13°
$B^- \to K_s \pi^-$	12.1	4,600	1		$< 4^\circ$ +
$B^o \to K^+ \pi^-$	18.8	62,100	20	γ	theory errors
$B^o \to \rho^+ \pi^-$	28	5,400	4.1		
$B^o \to \rho^o \pi^o$	5	780	0.3	α	$\sim 4^\circ$
$B_s \to J/\psi\eta$	330	2,800	15		
$B_s \to J/\psi\eta'$	670	9,800	30	$\sin(2\chi)$	0.024

$\dagger$ Can be used for a model dependent estimate of γ, see ref. [44].

improve the accuracy of the α determination [51]. We have not yet incorporated this idea.

- Although the $B \to K\pi$ modes provide the smallest experimental error in determining γ, there are model dependent errors associated with this method. On the other hand, two other methods, which use $B_s \to D_s^\pm K^\mp$ and $B^- \to \overline{D}^o K^-$, provide model independent results and can be averaged. The interplay of the three methods can be used to resolve ambiguities.

- The error in $\sin(2\chi)$ averaged over both $J/\psi\eta$ and $J/\psi\eta'$ decay modes of the B_s is ± 0.024. This translates to an error in the angle χ of 0.7°. Since χ is expected to be $\sim 2^\circ$, a precision measurement will take a few years if it is in the Standard Model range. Including $B_s \to J/\psi\phi$ can help reduce the time.

- The asymmetry in $B^o \to \pi^+\pi^-$ may be useful to gain insight into the value of α with theoretical input or combined with $B_s \to K^+K^-$ and theory to obtain γ. This study was done both with MCFast and GEANT. The signal efficiency is 10% higher in MCFast and the background levels the same in both, within statistics.

- The sign of $\cos(2\beta)$ can be determined in a few years without any theoretical assump-

tions using $B^o \to J/\psi K^o$, with $K^o \to \pi^{\pm}\ell^{\mp}\nu$, allowing the removal of two of the ambiguities in β. This reaction can also be used for CPT tests.

1.4.3 Sensitivity in Determining α Using $B^o \to \rho\pi$

1.4.3.1 Event Selection, Event Yields and Backgrounds

Here we give a detailed explanation of how the error in α was evaluated as an example of our analysis procedures as documented in the BTeV Proposal and the Proposal Update [53]. To measure α using $B^o \to \rho\pi$ requires the measurement of the tagged, time-dependent CP asymmetry in a particular combination of amplitudes obtained from a Dalitz plot analysis of the decay. The combination of amplitudes causes the Penguin terms to cancel and isolates the tree contribution to the decay, which provides the value of α. We have performed a Dalitz plot analysis that includes detector resolution and background along with the expected levels of detected signal events.

The reconstruction efficiencies for $B \to \rho\pi$ and backgrounds were studied using a full GEANT simulation, for $\rho^{\pm}\pi^{\mp}$ and $\rho^o\pi^o$, separately. All signal and background samples were generated with a mean of two interactions per crossing. relatively easy to generate, it is difficult to generate adequate samples of background events. For channels with branching ratio's of the order of 10^{-5}, it is necessary to generate $\sim 10^7$ events.

We look for events containing a secondary vertex formed by two oppositely charged tracks. One of the most important selection requirements for discriminating the signal from the background is that the events have well measured primary and secondary vertices. We demand that both the primary and the secondary have vertex fits with $\chi^2/dof < 2$. We also make a cut on the the distance between the primary and the secondary vertices, divided by the error, $L/\sigma_L > 4$. The two vertices must also be separated from each other in the plane transverse to the beam. We define $r_{transverse}$ in terms of the primary interaction vertex position (x_P, y_P, z_P) and the secondary decay vertex position (x_S, y_S, z_S) as $r_{transverse} = \sqrt{(x_P - x_S)^2 + (y_P - y_S)^2}$ and cut out events where the secondary vertex is close to the reconstructed primary. Furthermore, to insure that the charged tracks do not originate from the primary, we require that both the π^+ and the π^- candidate have an impact parameter with respect to the primary vertex (DCA) > 100 μm.

Events passing these selection criteria are searched for good π^o candidates. We select "bumps" in the calorimeter using cluster finder code that does the full pattern recognition. Photon candidates are required to have a minimum bump energy of 1 GeV and pass the shower "shape" cut which requires $E9/E25 > 0.85$, this selection is almost fully efficient on real electromagnetic showers and rejects backgrounds from hadronic interactions. We further reduce the background by ensuring that the photon candidates are not too close to the projection of any charged tracks on the calorimeter. For $\rho^{\pm}\pi^{\mp}$, the minimum distance requirement is > 2 cm, while for $\rho^o\pi^o$, we require the minimum distance > 5.4 cm. Candidate π^o's are two-photon combinations with invariant mass between 125 and 145 MeV/c^2. More details of π^o selection are given in the description of the analysis of the channel $B^o \to D^{*-}\rho^+$ in Section 16.3 of the 2002 Proposal.

Table 1.5: Selection Criteria

Criteria	$\rho^{\pm}\pi^{\mp}$	$\rho^0\pi^0$
Primary vertex criteria	$\chi^2 < 2$	$\chi^2 < 2$
Secondary vertex criteria	$\chi^2 < 2$	$\chi^2 < 2$
$r_{transverse}$ (cm)	0.0146	0.0132
Normalized distance L/σ	> 4	> 4
Distance L, cm	< 5	< 5
DCA of track, μm	> 100	> 100
t_{proper}/t_0	< 5.5	< 5.5
E_{π^+}, GeV	> 4	> 4
E_{π^-}, GeV	> 4	> 4
$p_t(\pi^+)$, GeV/c	> 0.4	> 0.4
$p_t(\pi^-)$, GeV/c	> 0.4	> 0.4
Isolation for γ, cm	> 2.0	> 5.4
E_{π^0}, GeV	> 5	> 9
$p_t(\pi^0)$, GeV/c	> 0.75	> 0.9
$\Delta p_t/\Sigma p_t$	< 0.06	< 0.066
m_{π^0}, MeV/c^2	$125 - 145$	$125 - 145$
m_ρ, GeV/c^2	$0.55 - 1.1$	$0.55 - 1.1$

Kinematic cuts greatly reduce the background to $B \to \rho\pi$ while maintaining the signal efficiency. Minimum energy and transverse momentum (p_t) requirements are placed on each of the three pions. Here p_t is defined with respect to the B direction which is defined by the position of the primary and secondary vertices. We demand that the momentum vector of the reconstructed B candidate point back to the primary vertex. The cut is implemented by requiring p_t balance among the π^+ plus π^-, and π^o candidates relative to the B-direction and then divided by the sum of the p_t values for all three particles ($\Delta p_t/\Sigma p_t$). We also make a cut on the B decay time requiring that the B candidate live no more than 5.5 proper lifetimes ($t_{proper}/t_0 < 5.5$). The selection criteria for the two modes are summarized in Table 1.5.

For this study, we generated and analyzed three large samples of events using BTeVGeant: 250,000 $B \to \rho^0\pi^0$ events, 250,000 $B \to \rho^+\pi^-$ events, and 9,900,000 generic $b\bar{b}$ background events. Background from minimum bias events has been shown to be negligible. The results of the analysis after applying the cuts in Table 1.5 are presented in Fig. 1.15 (for $\rho^o\pi^o$) and Fig 1.16 (for $\rho^+\pi^-$). The background mass spectra are on the left side of the figures, and the signal events are on the right side.

The mass resolution for the B is ≈ 28 MeV/c^2. The mean π^o mass value in the $B \to \rho\pi$ events is 135 MeV/c^2 with a resolution of about 3 MeV/c^2. The relevant yields for $\rho\pi$ are shown in Table 1.6. The reconstruction efficiency is $(0.18\pm0.01)\%$ for $\rho^0\pi^0$ and $(0.22\pm0.01)\%$ for $\rho^+\pi^-$. The background was obtained by considering the mass interval between 5 and 7 GeV/c^2. The signal interval is taken as $\pm2\sigma$ around the B mass or 112 MeV/c^2.

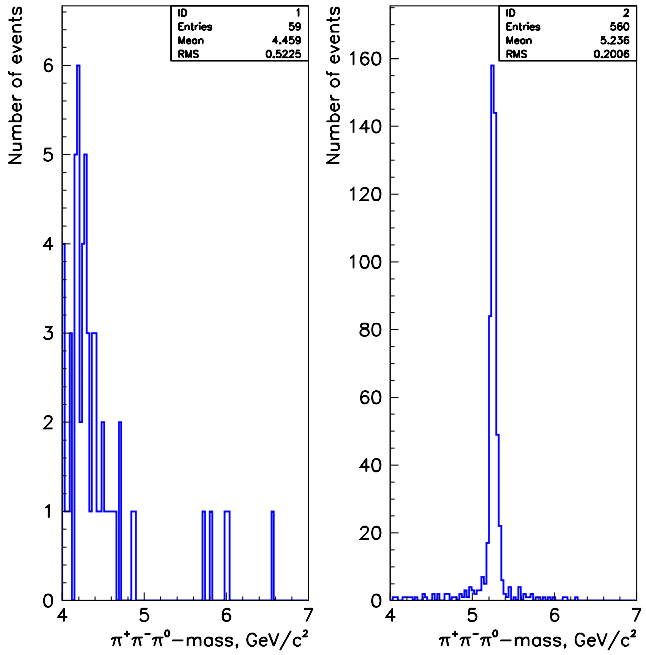

Figure 1.15: Invariant $\pi^+\pi^-\pi^o$ mass distributions for background (left) and signal (right) events for $B \to \rho^o\pi^o$.

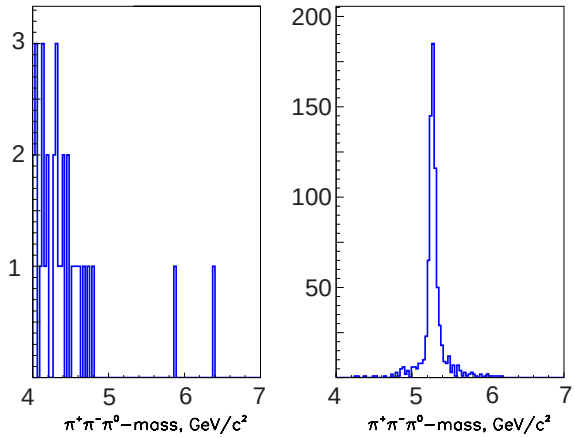

Figure 1.16: Invariant $\pi^+\pi^-\pi^o$ mass distributions for background (left) and signal (right) events for $B \to \rho^+\pi^-$.

Table 1.6: $B \to \rho\pi$ Yields

Quantity	$\rho^{\pm}\pi^{\mp}$	$\rho^o\pi^o$
Branching ratio	2.8×10^{-5}	0.5×10^{-5}
Efficiency	0.0022	0.0018
Trigger efficiency (Level 1)	0.7	0.7
Trigger efficiency (Level 2)	0.9	0.9
S/B	4.1	0.3
Signal/10^7 s	5,400	776
ϵD^2	0.10	0.10
Flavor tagged yield	540	78

The final numbers of both signal and background events are reduced by including the Level 1 and Level 2 trigger efficiency, but the S/B ratio is not significantly changed. From this study we find that we can expect to reconstruct 5,400 $\rho^{\pm}\pi^{\mp}$ events and 776 $\rho^o\pi^o$ events per year.

We can, therefore, expect to collect a sample of 540 flavor tagged $\rho^{\pm}\pi^{\mp}$ events and $\sim$78 $\rho^o\pi^o$ per year with signal-to-background levels of approximately 4:1 and 1:3, respectively.

1.4.3.2 Estimation of the Error on α

The decay amplitude may be written as

$$| B^0\rangle = f_+ a_{+-} + f_- a_{-+} + f_0 a_{00},$$

where $a_{i,j}$ refers to the three distinct final states as

$$a_{i,j} = a(B^0 \to \rho^i\pi^j),\ (i,j) = (+,-),(-,+),(0,0),$$

and f_k parameterizes the ρ decay amplitude. We use

$$f_k(s) = \frac{\cos\theta_k}{s - m_\rho^2 + i\prod(s)},$$

where θ_k is the angle between the direction of the B and the direction of a daughter pion, both viewed in the ρ rest frame, and s is the square of the dipion invariant mass $s = (E_{\pi_1} + E_{\pi_2})^2 - (\overrightarrow{p}_{\pi_1} + \overrightarrow{p}_{\pi_2})^2$; s can be in one of three charge states, s^+, s^- or s^o. In each case

$$\prod(s) = \frac{m_\rho^2}{\sqrt{s}}\left(\frac{p(s)}{p(m_\rho^2)}\right)^3 \Gamma_\rho(m_\rho^2),$$

p being the momentum in the ρ rest frame.

The amplitudes $a_{i,j}$ for B^o and $\overline{B^o}$ decay are written as a sum of Tree (T) and Penguin (P) parts as

$$a_{+-} = -e^{i\gamma}T^{+-} + e^{-i\beta}P^{+-}$$

$$a_{-+} = -e^{i\gamma}T^{-+} + e^{-i\beta}P^{-+}$$
$$a_{00} = -e^{i\gamma}T^{00} + e^{-i\beta}P^{00}$$
$$\bar{a}_{+-} = -e^{-i\gamma}T^{-+} + e^{i\beta}P^{-+}$$
$$\bar{a}_{-+} = -e^{-i\gamma}T^{+-} + e^{i\beta}P^{+-}$$
$$\bar{a}_{00} = -e^{-i\gamma}T^{00} + e^{i\beta}P^{00},$$

where γ and β are the usual CKM angles and $\alpha+\beta+\gamma = \pi$. Using both isospin symmetry and the fact that the Penguin amplitude is a pure $\Delta I = 1/2$ transition leads to the replacement

$$P^{00} = -\frac{1}{2}(P^{+-} + P^{-+}).$$

This leaves us with 9 parameters to be fit to the data including α, 3 complex Tree and 2 Penguin amplitudes, where one is defined as purely real and the total rate is used as an independent input. We can also allow the resonant and non-resonant background fractions to be determined by the fit, which adds two additional parameters.

For this study we used a data sample corresponding to 1.4 years of running (1.4×10^7s) with the one-arm version of BTeV. The background level is determined by a full GEANT simulation of 9,900,000 generic $b\overline{b}$ events; it is assumed that this background has an exponential time dependence given by the average lifetime of b-flavored hadrons. The background is parameterized with both resonant and non-resonant components. The non-resonant background is distributed uniformly over the Dalitz plot. The resonant background allows for two of the pions to have a Breit-Wigner shaped low mass enhancement. All charged tracks and photons in both signal and background events are smeared by the detector resolution before further analysis. Signal events are generated with an exponential time distribution modified by B^o mixing. The simulation is repeated for different assumptions about the relative size of Penguin and Tree amplitudes and the fraction of resonant and non-resonant background. For each set of data a maximum likelihood fit is performed where the likelihood is given by

$$-2\ln\mathcal{L} = -2\sum_{i=1}^{N_{B^o}} \ln\Bigg[\Big(\frac{\mid \mathcal{A}(s_i^+, s_i^-, t_i; \alpha, ..) \mid^2}{\mathcal{N}(\alpha, ..)} \times \varepsilon(s_i^+, s_i^-) +$$
$$R_{non} \times \frac{1}{\mathcal{N}_t} + R_{res} \times \frac{\mid \mathcal{BW}(s_i^+, s_i^-) \mid^2}{\mathcal{N}_{BW}} \times \varepsilon(s_i^+, s_i^-)\Big)/(1 + R_{non} + R_{res})\Bigg]$$
$$-2\sum_{j=1}^{N_{\overline{B}^o}} \ln\Bigg[\Big(\frac{\mid \bar{\mathcal{A}}(s_j^+, s_j^-, t_j; \alpha, ..) \mid^2}{\mathcal{N}(\alpha, ..)} \times \varepsilon(s_i^+, s_i^-) +$$
$$R_{non} \times \frac{1}{\mathcal{N}_t} + R_{res} \times \frac{\mid \mathcal{BW}(s_j^+, s_j^-) \mid^2}{\mathcal{N}_{BW}} \times \varepsilon(s_j^+, s_j^-)\Big)/(1 + R_{non} + R_{res})\Bigg],$$

where N_{B^o} and $N_{\overline{B}^o}$ are the total number of B^o and $\overline{B}^o$ events, respectively, and $\mathcal{N}$ is the normalization. It is given by $(\mid \mathcal{A} \mid^2 + \mid \bar{\mathcal{A}} \mid^2) \times \varepsilon$, integrated over the Dalitz plot acceptance, where ε is the detector efficiency. R_{non} and R_{res} are the ratios of non-resonant and resonant background to signal. For one case we show in Fig. 1.17 the χ^2 contours for α and correlations with the fractions of resonant and non-resonant backgrounds. The input value for α in this case was 77.3°. The fit has no trouble picking out the correct solution.

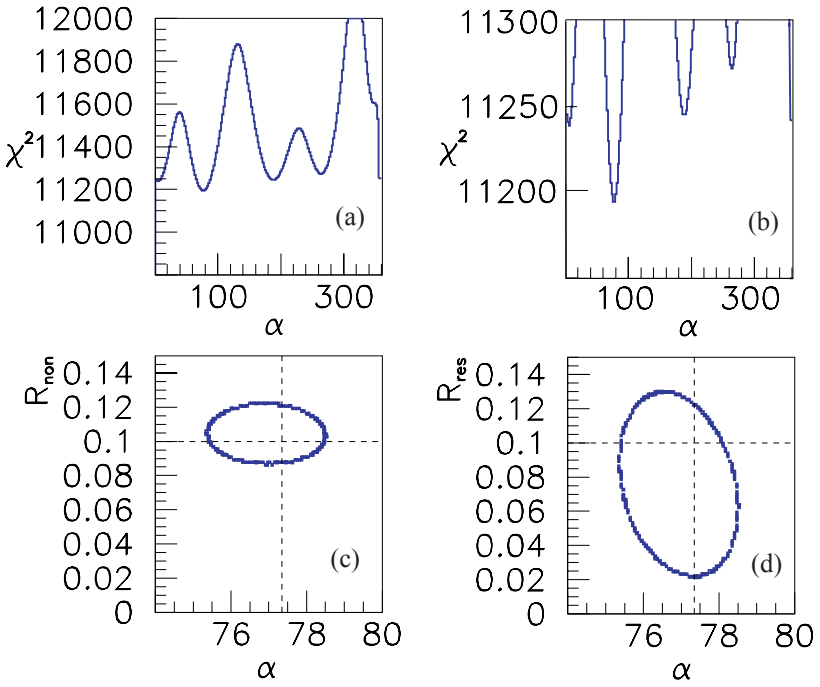

Figure 1.17: Results of a simulation using 1000 $B^o \to \rho\pi$ detected signal events with an input value of $\alpha = 77.3°$. (a) The χ^2 contours as a function of α. (b) same as (a) with the vertical scale enlarged. (c) The correlation of the best fit for α and R_{non} and (d) The correlation of the best fit for α and R_{res}.

Table 1.7 shows the results of an ensemble of fits with different assumptions on the fractions of resonant and non-resonant background, and different values of α. The one parameter fit assumes that the non-resonant and resonant background levels are determined from non-flavor tagged data, while in the three parameter fit, these are determined along with α.

These studies show that over a broad range of background models, α is determined with a sensitivity between 1.4°-4.3° in 1.4×10^7s of running time. The sensitivity will also depend on several unknown quantities including the branching ratio for $\rho^o\pi^o$, and the ratio of Tree to Penguin amplitudes, though this ratio has been inferred from the branching rates measured for two-body vector-pseudoscalar final states, and reasonable variations have already been included in these sensitivity estimates.

Table 1.7: Results of Determining α with 1000 $B^o \to \rho\pi$ Events.

α	Background, %		$\langle\alpha\rangle$	$\langle\sigma_\alpha\rangle$	$\langle\alpha\rangle$	$\langle\sigma_\alpha\rangle$
MC	Resonant.	Nonres.	1 parameter		3 parameters	
77.3	0	0	77.4	1.3	77.3	1.4
	10	10	77.4	1.4	77.3	1.5
	20	20	77.2	1.5	77.2	1.6
	40	0	77.4	1.6	77.2	1.8
	0	40	77.6	1.4	77.1	1.6
93.0	0	0	92.7	1.4	92.8	1.5
	10	10	93.3	1.6	93.4	1.8
	20	20	93.1	1.7	93.3	1.9
	40	0	92.7	1.8	93.2	2.1
	0	40	92.5	1.6	93.3	1.9
111.0	0	0	111.0	1.9	111.7	2.3
	10	10	110.7	2.3	110.6	3.6
	20	20	110.9	2.7	111.7	3.9
	40	0	111.2	2.8	110.4	4.3
	0	40	110.2	2.1	111.1	4.0

1.4.4 Sensitivity to B_s Mixing

BTeV can definitively reach x_s values of 75 in 2×10^7 seconds of running. Put another way, it will take us only 10 days of steady running to reach x_s of 20. These estimates are based on the decay mode $B_s \to D_s^+\pi^-$, with $D_s^+ \to \phi\pi^+$ and $K^{*o}K^+$. "Definitively" is used here to express the ability to make a measurement where the best solution for a fit to the oscillation frequency is better by "5 standard deviations" than the next best fit. Thus BTeV can cover the entire range of x_s values allowed in the Standard Model.

1.4.5 Sensitivities in New Physics Modes

Precision studies of b decays can bring a wealth of information to bear on new physics, that probably will be crucial in sorting out anything seen at the LHC. While there are many tests for New Physics that we can make, we will concentrate on a few representative decay modes.

1.4.5.1 Reach in Rare Decays

BTeV has excellent reach in rare decays. We have investigated the exclusive decays $B^o \to K^{*o}\mu^+\mu^-$, $B^+ \to K^+\mu^+\mu^-$ and the inclusive decay $B \to X_s\mu^+\mu^-$.

We acquire 2530 $K^{*o}\mu^+\mu^-$ decays in 10^7 seconds, with a signal/background of 11. This sample is enough to measure the lepton-forward-backward asymmetry and test the Standard Model. (We expect a similar number of $K^{*o}e^+e^-$ events, but since we have not simulated

these, we have not added them into our sample.) The Dalitz plot and forward-backward polarization are sensitive tests of New Physics. How sensitive they are depends on how much the New Physics differs from Standard Model expectations. In Fig. 1.18 we show the simulated data using the Standard Model expectation for the forward-backward asymmetry, assuming two years of dating taking using only $K^{*o}\mu^+\mu^-$ or one year if $K^{*o}e^+e^-$ are added in with the same acceptance. A fit to the data determines the location of the zero with a precision of 4%. This can be compared with the zero locations given in non-SM models as shown in Fig. 1.7 (unfortunately plotted here in terms of s, rather than $\sqrt{s}$).

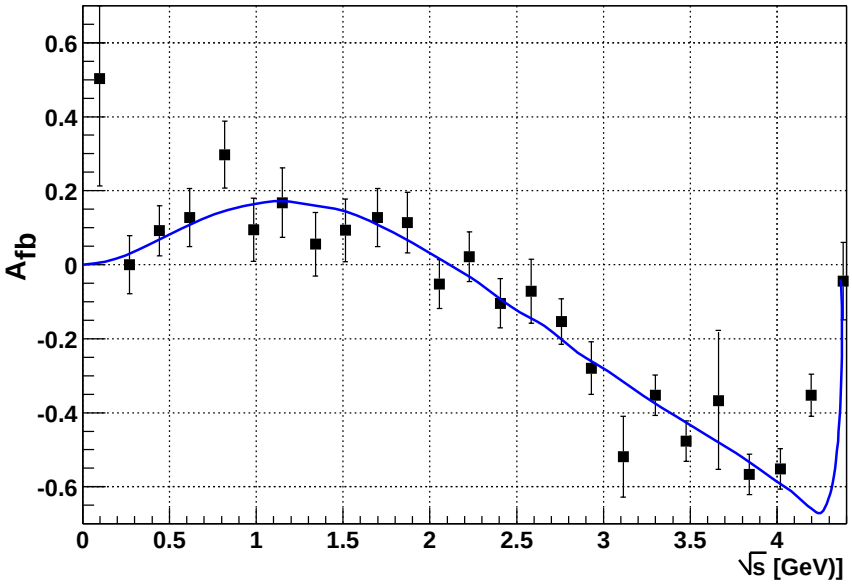

Figure 1.18: The normalized forward-backward asymmetry in $B \to K^*\mu^+\mu^-$ decay as a function of $\sqrt{s}$, the dilepton invariant mass. From ref. [54]

Although the asymmetry is expected to be small in $K^+\mu^+\mu^-$, we also test the Standard Model expectation, due to our large sample of ∼1300 events per year with a signal/background of 3.

We also expect to be able to measure the inclusive rate $b \to s\mu^+\mu^-$ with 20σ significance. This inclusive rate is very important. It could either show non-Standard Model physics or greatly constrain alternative models.

Other modes useful, for example, to test for Extra Dimensions are $B_s \to \mu^+\mu^-$ and $B_d \to \mu^+\mu^-$, where we expect totals of six and one event, respectively in 10^7 seconds, with signal/background above 10.

1.4.5.2 Reach in CP Violating Modes

The measurements described above of the CP violating angles and x_s already provide generic tests of New Physics. A large value of the angle χ, above ∼4°, would already provide prima facie evidence of New Physics.

Many other CP violating decay modes are also useful in detecting New Physics. In Table 1.8 we present our yields and the sensitivity in a few of these modes.

Table 1.8: BTeV Sensitivities in CP Violating Modes Pointed Toward New Physics for 10^7 seconds

Mode	$\mathcal{B} \times 10^{-6}$	Yield	S/B	parameter	error
$B^- \to \phi K^-$	6.9	11000	>10	CP asymmetry	0.01
$B^o \to \phi K_s$	3.45	2000	5.2	$\sin(2\beta)$	0.11
$D^{*+} \to \pi^+ D^o$; $D^o \to K^-\pi^+$	2.6×10^4	$\sim 10^8$	large	CP asymmetry	very small †

† Systematic error limited

The combination of measurements of all of these modes, the previous ones listed in Table 1.4 and many others than we can study with high statistics, will allow for a critical examination of any new physics found at the LHC.

1.5 Comparisons With Other Experiments

1.5.1 Comparison with e^+e^- B Factories

Much of what is known about b decays has been learned at e^+e^- machines [55]. Machines operating at the $\Upsilon(4S)$ found the first fully reconstructed B mesons (CLEO), B^o-$\overline{B}^o$ mixing (ARGUS), the first signal for the $b \to u$ transition (CLEO), and Penguin decays (CLEO). Lifetimes of b hadrons were first measured by experiments at PEP, slightly later at PETRA, and extended and improved by LEP [55].

The success of the $\Upsilon(4S)$ machines, CESR and DORIS, led to the construction at KEK and SLAC of two new $\Upsilon(4S)$ machines with luminosity goals in excess of $3 \times 10^{33}\mathrm{cm}^{-2}\mathrm{s}^{-1}$. These machines have asymmetric beam energies so they can measure time dependent CP violation. In fact, CP violation in B_d was convincingly demonstrated recently by both the BABAR and BELLE experiments [56]. These machines, however, will investigate only B^o and $B^\pm$ decays. They will not investigate B_s, B_c or Λ_b decays. While, in principle, the e^+e^- machines could run on the $\Upsilon(5S)$, which is likely to be a source of B_s mesons, there are crucial concerns that vitiate any such approach: The predicted cross-section for B_s production is only $\sim$0.1 of that of B production on the $\Upsilon(4S)$. Furthermore the proper time resolution necessary to resolve B_s oscillations cannot be obtained using the relatively slow B_s mesons produced at the $\Upsilon(5S)$.

Table 1.9 shows a comparison between BTeV and an asymmetric e^+e^- machine for measuring the CP violating asymmetry in the decay mode $B^o \to \pi^+\pi^-$. The peak luminosity for the e^+e^- machines is set at 10^{34} $\mathrm{cm}^{-2}\mathrm{s}^{-1}$, a value higher that what has been achieved. The detection and tagging efficiencies are taken from Aubert *et al.* [57]. In Table 1.10 we show a similar comparison for the final state $B^- \to \overline{D}^o K^-$, a mode that could be used to

determine the CKM angle γ. It is clear that the large hadronic b production cross section can overwhelm the much smaller e^+e^- rate. Furthermore, the e^+e^- B factories do not have access to the important CP violation measurements that need to be made in B_s decays. (See Table 1.11 for more comparisons.)

Table 1.9: Number of tagged $B^o \to \pi^+\pi^-$ ($\mathcal{B}$=0.45×10^{-5}).

	$\mathcal{L}(\mathrm{cm}^{-2}\mathrm{s}^{-1})$	σ	# $B^o/10^7$ s	Signal Efficiency	Tagging ϵD^2	# tagged/10^7 s
e^+e^-	10^{34}	1.1 nb	1.1×10^8	0.45	0.26	56
BTeV	2×10^{32}	100μb	1.5×10^{11}	0.021	0.1	1426

Table 1.10: Number of $B^- \to \overline{D}^o K^-$ ($\mathcal{B}$=1.7×10^{-7}).

	$\mathcal{L}(\mathrm{cm}^{-2}\mathrm{s}^{-1})$	σ	# $B^-/10^7$ s	Signal Efficiency	Events/10^7 s
e^+e^-	10^{34}	1.1 nb	1.1×10^8	0.4	5
BTeV	2×10^{32}	100μb	1.5×10^{11}	0.007	176

In Table 1.11 we show the expected rates in BTeV for one year of running (10^7 s) and an e^+e^- B-factory operating at the $\Upsilon(4S)$ with a total accumulated sample of 500 fb^{-1}, about what is expected before BTeV begins running.

1.5.2 Comments on Upgrades to KEK-B and PEP-II

Since late 1999, when PEP-II and KEK-B started, to end of Februray 2003, each machine delivered ∼110 fb^{-1} This corresponds to about 10^8 B^o mesons and 10^8 $B^{\mp}$ mesons produced for each experiment. The peak luminosity for PEP-II is around $5 \times 10^{33}\mathrm{cm}^{-2}\mathrm{s}^{-1}$, while KEK-B has achieved $8 \times 10^{33}\mathrm{cm}^{-2}\mathrm{s}^{-1}$.

KEK-B is planning on how to upgrade to a luminosity of $10^{35}\mathrm{cm}^{-2}\mathrm{s}^{-1}$, ten times their original design using the same machine configuration, with a target date of 2007. (Much of the reference material in this section comes from the E2 Snowmass working group report [58]. This document was signed by a representative cross-section of the community working on B physics.) However, as pointed out in the E2 report, the higher luminosity can cause problems for the detector: "Operation at 10^{35} has implications for the detector and the IR. The rates from collisions will be significantly higher which will lead to larger occupancy. Trigger rates and rates through the data acquisition system will be higher. There will be more synchrotron radiation, which will have to be removed by masking. There may be larger

Table 1.11: Comparison of BTeV yields in one year of running to the integrated yield of the asymmetric B Factories from 1999 to approximately 2007.

Mode	BTeV ($10^7 s$)			B-factory (500 fb^{-1})		
	Yield	Tagged†	S/B	Yield	Tagged†	S/B
$B_s \to J/\psi\eta^{(\prime)}$	12650	1645	>15			
$B^- \to \phi K^-$	11000	11000	>10	700	700	4
$B^o \to \phi K_s$	2000	200	5.2	250	75	4
$B^o \to K^{*o}\mu^+\mu^-$	2530	2530	11	∼50	∼50	3 [52]
$B_s \to \mu^+\mu^-$	6	0.7	> 15	0		
$B_d \to \mu^+\mu^-$	1	0.1	> 10	0		
$D^{*+} \to \pi^+ D^o$; $D^o \to K^-\pi^+$	$\sim 10^8$	$\sim 10^8$	large	8×10^5	8×10^5	large

† Tagged here means that the initial flavor of the B is determined.

vacuum pressure resulting in higher background rates from Touschek scattering. There may need to be a larger crossing angle which may make it harder to shield backgrounds efficiently. The final quads may be moved closer to the IP to reduce β^*. And finally, the background at injection might be significantly worse...the first few layers of the silicon vertex detector will have high occupancy and will be replaced by pixel detectors. Beampipe heating due especially to Higher Order Modes (HOM) requires that the beam pipe be water cooled. The Central Drift Chamber is undergoing a modification in 2002 to replace the two inner layers with a small cell chamber. It is expected to be able to handle super-KEK rates. The CsI(Tl) calorimeter is slow and something may need to be done to it. The RPCs in the muon system already suffer from inefficiency due to local deadtime and will probably need to be replaced with wire chambers. The data acquisition system will also have to be upgraded."

The Super-BABAR concept requires a new machine operating in either the PEP tunnel or the SLC arcs that achieves a luminosity of $10^{36}\text{cm}^{-2}\text{s}^{-1}$. According to the E2 Snowmass summary: "The goal is to be competitive with the next generation hadron collider experiments, at least in the area of B_d and B_u physics." However, in order to reach this goal, the machine must be successfully built and the detector essentially completely rebuilt to withstand the high rates and radiation load. The challenges for both the detector and the accelerator are enormous. Stu Henderson in his Snowmass summary talk said about machine: "Every parameter is pushed to the limit-many accelerator physics and technology issues [59]."

Concerning the detector, the E2 summary states: "Most of the BABAR subsystems will have to undergo some modification or replacement to handle the much higher rates of the new machine. To carry out the program, the overall performance, in terms of resolution, efficiency, and background rejection, must be similar to that of BABAR. The detector must retain its high degree of hermeticity as well.

"There are many questions about the cost and availability of suitable detector technologies which will need to be studied before the detector design can be finalized. We give four

examples. (1) To maintain the vertex resolution of BABAR and withstand the radiation environment, pixels with a material budget of 0.3% X_o per layer are proposed. Traditional pixel detectors which consist of a silicon pixel array bump-bonded to a readout chip are at least 1.0% X_o. To obtain less material, monolithic pixel detectors are suggested. This technology has never been used in a particle physics experiment. (2) As a drift chamber cannot cope with the large rates and large accumulated charge, a silicon microstrip tracker has been proposed. At these low energies track parameter resolution is dominated by multiple Coulomb scattering. Silicon microstrip technology is well tested but is usually used at this energy for vertexing, not tracking. Realistic simulations need to be performed to establish if momentum resolution as good as BABAR can be achieved with the large amount of material present in the silicon tracker. If not, we suggest a TPC, possibly readout with a Gas Electron Multiplier, or MICROMEGAS, be explored as an alternative to the silicon tracker (3) There is no established crystal technology to replace the CsI(Tl). There are some candidate materials but the most attractive have not been used in a calorimeter previously. (4) There is no known technology for the light sensor for the SuperDIRC.

"Since the goal of the SuperKEK and SuperBABAR upgrades are to enable the e^+e^- machine to compete with future hadron collider experiments, it is important to make a realistic evaluation of the sensitivities of all these experiments over a wide range of final states. Such projections are, of course, somewhat uncertain. The sensitivities of future hadron collider experiments have been determined from detailed and sophisticated simulations of signals and backgrounds. As these simulations are an approximation to reality, the performance of LHCb and BTeV may be somewhat better or somewhat worse than the simulations predict. Projections for SuperBABAR are, at this point, mainly done by scaling from BABAR experience assuming that the new detector, which still has many open R&D issues, will achieve the same efficiency that BABAR now achieves even though the luminosity will be a factor of 300 higher. More realistic studies need to be performed before a full comparison between SuperBABAR and the hadron collider experiments is made. With these caveats a comparison of BTeV, LHCb, BABAR and Belle in 2005, and the e^+e^- machines at 10^{35} and 10^{36} is given in Table 1.12 for several states of importance to the study of *CP* violation in B decays."

This study indeed demonstrates that it will take a $10^{36} cm^{-2} s^{-1}$ e^+e^- *collider operating at the* $\Upsilon(4S)$ *to match the performance of BTeV on* B^o *and* $B^{\mp}$ *mesons, while there will be no competition for the* B_s *or other b-flavored hadrons. There are serious technical problems that both the machine and the detector would need to surmount. We believe the cost will far exceed that of BTeV. The HEPAP subpanel in their report [60] mentions a 500 M$ number for the detector. That cost has not been subject to review.*

We note that the LHCb sensitivity for $\sin 2\alpha$ is quoted as 0.05, the same as BTeV even though BTeV gathers twice as many events and has a much better signal to background (see section 1.5.4.2 for a more detailed comparison and section 1.4.3.2 for the BTeV analysis). This LHCb number comes from P. Ball *et al.* [61] where these caveats are included: "It should be stressed that the fitting studies are preliminary and are optimistic in the fact that the exact LHCb acceptance has not been used and the backgrounds have not been included..."

Table 1.12: Comparison of CP Reach of Hadron Collider Experiments and SuperBABAR. The last column is a prediction of which kind of facility will make the dominant contribution to each physics measurement. (From the E2 summary [58].)

	BTeV† 10^7s	LHCb 10^7s	BABAR Belle (2005)	e^+e^- 10^{35} 10^7s	e^+e^- 10^{36} 10^7s	e^+e^- at 10^{36} vs hadron collider
$\sin 2\beta$	0.017	0.02	0.037	0.026	0.008	Equal
$\sin 2\alpha$	0.05	0.05	0.14	0.1	0.032	Equal
$\gamma\,[B_s(D_sK)]$	$\sim 8^o$					Had
$\gamma\,[B(DK)]$	$\sim 13^o$		$\sim 20^o$		12^o	Equal
$\sin 2\chi$	0.024	0.04	-	-	-	Had
$\mathcal{B}(B \to \pi^o\pi^o)$	-	-	$\sim$20%	14 %	6%	e^+e^-
V_{ub}	-	-	$\sim$2.3%	$\sim$1% (sys)	$\sim$1% (sys)	e^+e^-

† We have changed the BTeV numbers to correspond to the one-arm section 1.4.3.2.

1.5.3 Comparisons with CDF and D0

Both CDF and D0 have measured the b production cross section [62]. CDF has contributed to our knowledge of b decay mostly by its measurements of the lifetime of b-flavored hadrons [63], which are competitive with those of LEP [64] and recently through its discovery of the B_c meson [65]. CDF also saw the first hint for CP violation in the b system [66]. These detectors were designed for physics discoveries at large transverse momentum. It is remarkable that they have been able to accomplish so much in b physics. They have shown that it is possible to do b physics in the environment of a hadron collider. We expect that a measurement of B_s mixing will be performed at the Tevatron before BTeV turns on.

These detectors, however, are very far from optimal for b physics. BTeV has been designed with b physics as its primary goal. To have an efficient trigger based on separation of b decays from the primary, BTeV uses the large rapidity region where the b's are boosted. The detached vertex trigger allows collection with very high efficiency of interesting purely hadronic final states such as $\pi^+\pi^-$, $\rho\pi$, $D_s^+\pi^-$ and $D_s^+K^-$. It is also efficient for an eclectic mixture of all b decays and is therefore open to decays which may not be considered "interesting" now or at the time of data taking, but may become so as our knowledge improves. It also allows us to collect enough charm to investigate charm mixing and CP violation.

The use of the forward geometry also allows for excellent charged hadron identification over a wide momentum range, with a gaseous RICH detector. This is crucial for many physics issues such as separating $K\pi$ from $\pi\pi$, $D_s\pi$ from D_sK, kaon flavor tagging, etc. CDF has some particle identification using dE/dx in the drift chamber and now has a time-of-flight system, but the TOF cannot separate kaons from pions above momenta of $\sim$1 GeV/c, much too low for most of the decay products of low multiplicity B decays, but useful for flavor tagging, where the momenta are lower. The particle identification power of BTeV allows,

for example, a vast reduction in background for the final states $B_s \to D_s^{\pm} K^{\mp}$, $B^- \to \overline{D}^o K^-$ and $B^o \to \pi^+\pi^-$, compared with CDF or D0, as documented in ref. [67], and which allows BTeV to make precise measurements in these modes. For example, in $\overline{B}_s \to D_s^+ K^-$ the BTeV signal/background is 7:1, while its 1:6 in CDF.

Furthermore an experiment that plans on answering all the open questions in b physics, requires a high quality electromagnetic calorimeter. Installation of such a calorimeter in the CLEO detector made new physics vistas possible and such a device in BTeV allows for the measurement of several crucial final states such as $B^o \to \rho\pi$, and $B_s \to J/\psi\eta'$.

Finally, BTeV has all the crucial elements required to study any newly suggested b or charm process or uncover new physics. The crucial elements are:

- a detached vertex algorithm in the first trigger level,
- highly efficient particle identification across the entire momentum range with good ($\approx$50:1) background rejection,
- an electromagnetic calorimeter with sufficiently good energy resolution and efficiency to fully reconstruct rare B decay final states with single photons or neutral pions.

BTeV will have a physics reach substantially beyond that of CDF, and D0, and for that matter of CMS, and ATLAS. The sensitivities of CDF and D0 are summarized in Anikeev *et al.* [67] and those of CMS and ATLAS in Ball *et al.* [61].

1.5.4 Comparisons with LHCb

1.5.4.1 General Comparisons

LHCb [68] is an experiment planned for the LHC with almost the same physics goals as BTeV. BTeV is at least as good as LHCb in all areas and it is far superior in some very important areas. Both experiments intend to run at a luminosity of 2×10^{32} cm^{-2}s^{-1}. There are several inherent advantages and disadvantages that LHCb has compared with BTeV. The issues that favor LHCb are:

- The b production cross-section is expected to be about five times larger at the LHC than at the Tevatron, while the total cross-section is only 1.6 times as large.
- The mean number of interactions per bunch crossing is expected to be about 3 times lower at the LHC than at the Tevatron.

The issues that favor BTeV are:

- BTeV has to cover a smaller range of particle momenta. The seven times larger beam energy at the LHC makes the momentum range of particles that need to be tracked and identified much larger and therefore more difficult. The larger energy also causes a large increase in track multiplicity per event, which makes pattern recognition and triggering more difficult.

- The interaction region at the Tevatron is three to six times longer along the beam direction than at LHC ($\sigma_z = 5$ cm), which allows BTeV to be able to accept collisions with a mean of up to six interactions per crossing, since the interactions are well separated in z. LHCb planned until quite recently to veto crossings with more than one interaction.

- The short bunch spacing at the LHC, 25 ns, has serious negative effects on all their detector subsystems. There are occupancy problems if the sub-detector integration times are long. This can be avoided by having short integration times, but that markedly increases the electronics noise. For example, in a silicon detector these considerations make first level detached vertex triggering more difficult than at the Tevatron; BTeV will have a beam crossing interval that is no shorter than a relaxed 132 ns, at least 5.3 times longer. In fact, LHCb's plan is to trigger in their first trigger level on muons, electrons or hadrons of moderate p_t, and detect detached vertices in the next trigger level. For two-body decays, they now believe only the p_t trigger is sufficient.

- BTeV is designed to have the vertex detector in the magnetic field, thus allowing the rejection of low momentum tracks at the trigger level. Low momentum tracks are more susceptible to multiple scattering which can cause false detached vertices leading to poor background rejection in the trigger. LHCb has recently recognized this flaw in their design. They have removed the shielding plate on their magnet and now have a magnetic field between 50 and 260 Gauss on their vertex detector. Unfortunately this also puts 250-1000 Gauss on their first RICH detector, which causes the tracks to bend while traversing the gas radiator and we believe will significantly detoriate the resolution. It also makes it very difficult to shield the HPD photon-detectors.

- BTeV is designed with a high quality $PbWO_4$ electromagnetic calorimeter, that provides high resolution and acceptance for interesting final states with γ's, π^o's, and $\eta^{(\prime)}$'s. The BTeV electromagnetic calorimeter is superior in energy resolution and segmentation to LHCb's. LHCb has a Shaslik-style Pb-scintillating fiber device, following a preshower detector. The LHCb energy resolution is $10\%/\sqrt{E} \oplus 1.5\%$, which compares poorly with BTeV's $1.7\%/\sqrt{E} \oplus 0.55\%$. The LHCb detector segmentation is 4 cm $\times$ 4 cm up to $\sim$90 mr, 8 cm $\times$ 8 cm to $\sim$160 mr and 16 cm $\times$ 16 cm at larger angles. (The distance to the interaction point is 12.4 m.) Thus the segmentation is comparable to BTeV only in the inner region. (BTeV has 2.8 cm $\times$ 2.8 cm crystals 7.4 m from the center of the interaction region.)

- Use of a detached vertex trigger at Level 1 allows for an extensive charm physics program absent in LHCb. It also accepts a more general collection of b events, which are less oriented towards particular final states.

- The LHCb data acquisition system is designed to output 200 Hz of b decays, while BTeV is designed for larger output bandwidth of 1,000 Hz of b's and 1,000 Hz of charm, and

an additional 2000 Hz for contingency, calibration events, and other physics. Therefore, BTeV has access to a much wider range of heavy quark decays.

We have compensated for LHCb's initial advantages in b cross-section due their higher center-of-mass energy. In fact, the high energy actually works in many ways as a disadvantage. For example, LHCb needs two RICH counters to cover the momentum range in their one arm. Particle identification and other considerations force LHCb to be longer than BTeV, in fact about twice as long. As a result, LHCb's transverse area is four times that of BTeV, in order to cover the same solid angle. It is expensive to instrument all of this real estate with high quality particle detectors. Thus, the total cost for LHCb based only on instrumented area, (a naive assumption) would be four times the total cost for BTeV.

For our Proposal and Proposal Update, we compared our physics reach with that of LHCb as documented in their Technical Design Report [68] and a B Physics at the LHC document [61]. Recently, however, they have extensively redesigned their detector and now call it "LHCb Light" [69]. The changes were prompted at least partially by them not using the proper Pythia generator (they were using version 5.7 rather than 6.2, while BTeV always used 6.2) and their realization that they had too much material in the upstream part of the detector. The changes include reducing the number of silicon strip detectors in their vertex detector from 25 to 21 and lowering the silicon thickness from 300 to 220 μm; reducing the number of tracking stations; removing the magnet shielding plate, thus allowing field on the vertex detector and RICH-1; allowing triggers on multiple interactions in each crossing; and adding a high p_t only trigger which helps primary on $B \to h^+h^-$ final states.

While LHCb has computed efficiencies in this new configuration, they have not simulated enough background events so that their background levels are not known and furthermore our experience is that you may have to drastically retune your signal selections when you find out about the backgrounds you have to fight, and this could materially lower their efficiencies. We are particularly concerned that in "LHCb Light" their ghost track rate on tracks going through the entire spectrometer is between 8-16%, depending on p_t, while BTeV ghost rate is less than 1% for similar tracking efficiency of 95%.

Therefore, we cannot do an up-to-date detailed comparison between BTeV and LHCb. However, we will reproduce our comparisons with their Technical Proposal, assuming that they will reach this level of performance with "LHCb Light." We use three modes of great importance because they give direct determinations of the CP violating angles α, χ and γ.

1.5.4.2 A Specific Comparison: $B^o \to \rho\pi$

We base our comparison on the total number of untagged events quoted by both experiments. All rates are calculated for 10^7 seconds at a luminosity of 2×10^{32} cm^{-2}s^{-1}. We have corrected the LHCb numbers by normalizing them to the branching ratios used by BTeV. In Table 1.13 we compare the relevant quantities [70].

LHCb has done a background estimate based on a heavily preselected sample of events [71]. These include:

Table 1.13: Event yields and signal/background for $B^o \to \rho\pi$.

Mode	Branching Ratio	BTeV		LHCb	
		Yield	S/B	Yield	S/B
$B^o \to \rho^{\pm}\pi^{\mp}$	2.8×10^{-5}	5400	4.1	2140	0.8
$B^o \to \rho^o\pi^0$	0.5×10^{-5}	776	0.3	880	-

- a preselection for charged pions and photons which required the momentum or energy to exceed a value depending on the polar angle of the candidate. For charged pions, the momentum cut varied between 1 and 2 GeV/c and for photons the energy cut varied between 2 and 6 GeV;
- selection of signal-like events based on a discriminant variable built from kinematic variables of the π, ρ and B^o;
- selection based on the reconstructed secondary vertex for a $\pi^+\pi^-$ combination; and
- Dalitz plot cuts to eliminate low energy π^o combinatorial background due to particles from the primary vertex.

These cuts are applied to the generator event sample before the events are processed through GEANT [72]. The BTeV simulation was carried out without any preselection cuts. We were worried that the preselection would bias us to lower background rates. For example, if two photons overlapped or interactions of charged tracks put energy into photon clusters these can well become part of our background sample. Thus the LHCb background estimate may well be only a lower limit.

We note that their π^o mass resolution varies between 5 and 10 MeV/c^2 (r.m.s.) and their B^o mass resolution is 50 MeV/c^2 (r.m.s.). The corresponding numbers for BTeV are 3.1 MeV/c^2 and 28 MeV/c^2.

With this analysis, LHCb claims signal/background (S/B) of 1.3 for $\rho^{\pm}\pi^{\mp}$, where they have assumed a branching ratio of 4.4×10^{-5}. For our assumed branching ratio, S/B is 0.8; The S/B for BTeV is 4.1. Furthermore, the BTeV background analysis was done without preselection and therefore is likely to be more realistic. For the final state $\rho^o\pi^o$ LHCb has not produced a background estimate; in our experience it is difficult to estimate signal efficiencies without evaluating how restrictive the selection criteria need to be to reduce backgrounds.

It is not surprising that BTeV's superior crystal calorimeter and detached vertex trigger produce a large advantage in this final state over LHCb, even using LHCb's optimistic numbers. BTeV has a factor of 2.2 advantage in signal yield in $\rho^{\pm}\pi^{\mp}$ and a better S/B by a factor of 5. This results in an advantage to BTeV in the number of "effective events" (events weighted by dilution due to background) of almost a factor of 4.

1.5.4.3 A Specific Comparison: $B_s \to D_s^{\pm} K^{\mp}$

A comparison of the estimated total efficiencies (excluding D_s decay branching ratios), B_s mass resolutions, and S/B ratios are given in Table 1.14. Here $D_s^+ \to K^+K^-\pi^+$ can be reconstructed via either $\phi\pi^+$ or $K^{*o}K^-$. Here BTeV and LHCb differ somewhat. LHCb has the same efficiency in both modes, whereas BTeV analyzes them somewhat differently. For $K^{*o}K^-$ BTeV requires both charged kaons to hit the RICH detector, while for $\phi\pi^+$ only one charged kaon is required to be identified in the RICH. (The reconstruction efficiency for $\phi\pi^+$ is 2.3%, while for $K^{*o}K^-$ it is 1.3%).

Table 1.14: Comparison of BTeV and LHCb sensitivities for $B_s \to D_s^{\pm} K^{\mp}$.

Branching Ratio	BTeV		LHCb	
	Yield	S/B	Yield	S/B
3×10^{-4}	7,530	7	7,660	7

The yields and signal/background are about the same in this mode. This is not unexpected. The LHCb trigger efficiency is 4.1 times lower than BTeV and the acceptances are about equal. This factor of 4 should neutralize the LHCb cross-section advantage, of a factor of 5, and in this study it has.

1.5.4.4 A Specific Comparison: Measurement of χ

LHCb because of their relatively poor Electromagnetic Calorimeter LHCb must rely on the vector-vector final state in the reaction $B_s \to J/\psi\phi$. Here the sensitivity is related to several questions beyond the event yields and signal to background. The final state particles are in both CP + and CP - final states and the sensitivity is a sharp function of this ratio. The sensitivity also depends on knowing $\Delta\Gamma$, the difference in widths between the two CP states. LHCb claims that with precise knowledge of $\Delta\Gamma$ and a favorable ratio of CP eigenstates, namely that one is dominant, that they will be able to measure χ to about 1.5° in one year. Using the CP eigenstates $B_s \to J/\psi\eta^{(\prime)}$ alone, BTeV's error is 0.7° and BTeV can add in the $J/\psi\phi$ mode if it is at all useful. Moreover, BTeV can use its lifetime measurements in $J/\psi\eta^{(\prime)}$, a CP + final state combined with the lifetime in the mixed $D_s^+\pi^-$ final state to get a measurement of $\Delta\Gamma$, and thus provide useful information for the analysis of CP violation in the $J/\psi\phi$, which can lead to the removal of ambiguities in χ and ambiguities in γ using other final states.

1.5.5 Summary of Comparisons

BTeV has all the proper elements to make it the "best of breed" heavy quark experiment. It has a relatively unbiased vertex trigger that allows it to accumulate b and c quark events at

unprecedented rates. Like the B-factories it has both excellent charged particle identification and photon detection. Furthermore it is coupled to a prolific source of b and c quarks that permits the experiment to collect 1 kHz of b's and 1 kHz of charm. BTeV will make the best measurements in the world on the important CKM angles α using $B^o \to \rho\pi$, γ using $B_s \to D_s^{\pm} K^{\mp}$ and χ using $B_s \to J/\psi\eta^{(\prime)}$.

BTeV is far superior to current e^+e^- colliders operating on the $\Upsilon(4S)$ because of the enormous difference in the b rate. For reconstructed B^+ and B^o decays, BTeV has a factor of $\sim$200 more rate. Furthermore, the important B_s physics cannot be done at the e^+e^- machines. A luminosity on the order of $10^{36}\mathrm{cm}^{-2}\mathrm{s}^{-1}$ would need to be achieved before these machines would be competitive in B^o and $B^{\pm}$ physics with BTeV. It is of crucial importance the decay time resolution in BTeV is about 45 fs, for most final states, which compares most favorably to the 900 fs in asymmetric e^+e^- colliders. The studies presented here were done on what is currently believed to be the most important modes. What's in fashion, however, changes. BTeV is a powerful enough detector to be able to test new and interesting ideas for all b species.

CDF, and D0 cannot compete in areas where particle identification or photon detection are important; as a result, the b-physics reach of BTeV is substantially greater.

BTeV is competitive with LHCb in 'high-priority' final states with all charged particles. For final states with γ's, π^o's, η's or η''s, BTeV has a factor of $\approx$4 advantage. Furthermore, BTeV will write to tape a factor of 5 more b events than LHCb, allowing for more physics studies. This is of particular importance because there are many new ideas in this field where new decay modes are "discovered" to be of particular value. BTeV will have these on "tape," while LHCb is only 1/5 as likely to also have them in the b sector, and far less likely in the charm sector.

Therefore, BTeV is the best detector to discover New Physics or provide crucial information necessary for deciphering any New Physics found at the LHC.

Bibliography

[1] M. B. Gavela, P. Hernández, J. Orloff and O. Pène O, *Mod. Phys. Lett.* **A 9**, 795 (1993) [hep-ph/9312215].

[2] J. Ellis, Nucl. Phys. Proc. Suppl. **99A**, 331 (2000) [hep-ph/0011396].

[3] M. Kobayashi and K. Maskawa *Prog. Theor. Phys.* 49, 652 (1973).

[4] L. Wolfenstein *Phys. Rev. Lett.* 51, 1945 (1983).

[5] J. P. Silva, L. Wolfenstein, *Phys. Rev.* **D 55**, 5331 (1997) [hep-ph/9610208].

[6] R. Aleksan, B. Kayser and D. London, *Phys. Rev. Lett.* **73**, 18 (1994) [hep-ph/9403341].

[7] I. I. Bigi and A. I. Sanda, "On the Other Five KM Triangles," [hep-ph/9909479].

[8] Y. Nir, " CP Violation: The CKM Matrix and New Physics ," Plenary talk given at the 31st international conference on high energy physics (ICHEP 2002), Amsterdam, 24-31 July 2002, [hep-ph/0208080].

[9] A. Hocker *et al.*, *Eur. Phys. J.* **B435**, 427 (1998).

[10] M. E. Peskin, "Theoretical Summary Lecture for EPS HEP99," to appear in proceedings [hep-ph/0002041].

[11] F. J. Greub, A. Ioannissian and D. Wyler, *Phys. Lett.* **B 346**, 149 (1995) [hep-ph/9408382].

[12] A. Masiero and O. Vives, "New Physics Behind the Standard Model's Door?," Int. School on Subnuclear Physics, Erice, Italy, 1999 [hep-ph/0003133].

[13] Y. Nir, "CP Violation In and Beyond the Standard Model," IASSNS-HEP-99-96 [hep-ph/9911321] (1999).

[14] I. Hinchliff and N. Kersting, "Constraining CP Violating Phases of the MSSM," *Phys. Rev.* **D 63**, 015003 (2001) [hep-ph/0003090].

[15] R. A. Briere *et al.*, *Phys. Rev. Lett.*, **86**, 3718 (2001) [hep-ex/0101032].

[16] B. Aubert *et al.*, *Phys. Rev. Lett.*, **87**, 151801 (2001) [hep-ex/0105001].

[17] A. Ali *et al.*, *Phys. Rev.* **D 61**, 074024 (2000) [hep-ph/9910221].

[18] A. Ali *et al.*, *Phys. Rev.* **D 66**, 034002 (2002) [hep-ph/0112300.

[19] D. Chakraverty, K. Huitu and A. Kundu, "Effects of Universal Extra Dimensions on B^o Mixing," [hep-ph/0212047; J. Kubo and H. Terao, Suppressing FCNC and CP-Violating Phases with Extra Dimensions [hep-ph/0211180]; S. J. Huber, "Flavor Physics and Warped Extra Dimensions," [hep-ph/0211056]; K. Agashe, N. G. Deshphande and G. H. Wu, "Universal Extra Dimensions and $b \to s\gamma$," *Phys. Lett.* **B 514**, 309 (2001) [hep-ph/0105084]; G. Barenboim, F. J. Botella and O. Vives, "Constraining Models With Vector-Like Fermions from FCNC in K and B Physics," *Nucl. Phys.* **B 613**, 285 (2001) [hep-ph/01050306]; G. C. Branco, A. de Gouvea and M. N. Rebelo, "Split Fermions in Extra Dimensions and CP Violation," *Phys. Lett.* **B 506**, 115 (2001) [hep-ph/0012289]; D. Chang, W. Y. Keung and R. N. Mohapatra, "Models for Geometric CP Violation With Extra Dimensions," *Phys. Lett.* **B 515**, 431 (2001) [hep-ph/0105177]; J. Papavassiliou and A. Santamaria, "Extra Dimensions at the One Loop Level: $Z \to b\overline{b}$ and $B - \overline{B}$ Mixing," *Phys. Rev.* **D 63**, 016002 (2001) [hep-ph/016002].

[20] A. Aranda and J. Lorenzo Diaz-Cruz, "Flavor Symmetries in Extra Dimensions," [hep-ph/0207059].

[21] A. J. Buras, M. Spranger and A. Weiler, "The Impact of Universal Extra Dimensions on the Unitarity Triangle and Rare K and B Decays," [hep-ph/0212143].

[22] T. Applequist, H.C. Cheng and B. A. Dobrescu, *Phys. Rev. D* **64**, 035002 (2001) [hep-ph/0012100].

[23] D. Chang, A. Masiero and H. Murayama, "Neutrino mixing and large CP violation in B physics," [hep-ph/0205111].

[24] L. Wolfenstein and Y.L. Wu, *Phys. Rev. Lett.* **74**, 2809 (1994) [hep-ph/9410253].

[25] G. Buchalla, G, Hiller, and G. Isidori, *Phys. Rev.* **D 63**, 014015 (2000) [hep-ph/0006136].

[26] I. Hinchliff and N. Kersting, "CP Violation from Noncommutative Geometry," LBNL-47750 [hep-ph/0104137].

[27] A. Bartl, *et al.*, *Phys. Rev.* **D 64**, 076009 (2001) [hep-ph/0103324].

[28] A. Ali, G. Kramer and C. D. Lu, *Phys. Rev.* **D 59**, 014005 (1999) [hep-ph/9805403].

[29] B. Kayser, "Cascade Mixing and the CP-Violating Angle Beta," [hep-ph/9709382]. Previous work in this area was done by Y. Azimov, *Phys. Rev.* **D 42** (1990) 3705.

[30] A. Dighe, I. Dunietz and R. Fleischer, *Phys. Lett.* **B 433**, 1998 (147) [hep-ph/9804254].

[31] A. E. Snyder and H. R. Quinn, *Phys. Rev.* **D 48** (1993) 2139.

[32] C. P. Jessop *et al.* (CLEO), *Phys. Rev. Lett.*, **85**, 2881 (2000) [hep-ex/0006008].

[33] M. Bona, BABAR preprint BABAR-CONF-01/71, SLAC-PUB-9045 [hep-ex/0107058].

[34] A. Gordon *et al.* (Belle), *Phys. Lett. B*, **542**, 183 (2002) [hep-ex/0207007].

[35] A. Ali, G. Kramer, and C.D. Lu, *Phys. Rev.* **D 59**, 014005 (1999) [hep-ph/9805403].

[36] Y. Grossman and H. R. Quinn, *Phys. Rev.* **D 56**, 7259 (1997) [hep-ph/9705356].

[37] D. Du, I. Dunietz and Dan-di Wu, *Phys. Rev* **D 34**, 3414 (1986); R. Aleksan, I Dunietz, and B. Kayser, *Z. Phys.* **C 54**, 653 (1992); R. Aleksan *et al.*, *Z. Phys.* **C 67**, 251 (1995) [hep-ph/9407406].

[38] D. Atwood, I. Dunietz and A. Soni, *Phys. Rev. Lett.* **78**, 3257 (1997).

[39] M. Gronau and D. Wyler, *Phys. Lett.* **B 265**, 172 (1991).

[40] R. Fleischer and T. Mannel, *Phys. Rev.* **D 57**, 2752 (1998) [hep-ph/9704423].

[41] M. Neubert and J. L. Rosner, *Phys. Rev. Lett.* **81**, 5076 (1998) [hep-ph/9809311].

[42] A. J. Buras and R. Fleischer, "Constraints on γ and Strong Phases from $B \to \pi K$ Decays," presented at ICHEP 2000, Osaka, Japan, July 2000. To appear in the Proceedings [hep-ph/0008298].

[43] M. Beneke, G. Buchalla, M. Neubert and C. T. Sachrajda, "QCD factorization for $B \to \pi K$ decays," Contribution to ICHEP 2000, July 2000, Osaka, Japan, to appear in the Proceedings [hep-ph/0007256].

[44] R. Fleischer, *Eur. Phys. J.* **C10** 299, 1999.

[45] G. Hiller, "Physics Reach of Rare B Decays," [hep-ph/0207121].

[46] A. Masiero and O. Vives, New Physics in CP Violation Experiments, *Ann. Rev. of Nucl. & Part. Science* **51**, (2001) [hep-ph/0104027].

[47] V. Kostelecky and R. Van Kooten, *Phys. Rev. D*, **54**, 5585 (1996) [hep-ph/9607449]; Dong-Sheng Du and Zheng-Tao Wei, *Eur. Phys. J.*, **C14**, 479 (2000) [hep-ph/9904403]; L. Lavoura, *Phys. Rev. D*, **62**, 056002 (2000) [hep-ph/9911209], and references cited therein.

[48] http://www-btev.fnal.gov/DocDB/0000/000066/002/index.html

[49] I. Dunietz, *Phys. Lett.* B **427**, 179 (1998) (hep-ph/9712401).

[50] A. E. Snyder and H. R. Quinn, *Phys. Rev. D* **48** (1993) 2139.

[51] H. R. Quinn and J. P. Silva, "The Use of Early Data on $B \to \rho\pi$ Decays," hep-ph/0001290 (2000).

[52] K. Abe *et al.*, *Phys. Rev. Lett.* **88**, 021801 (2002) (hep-ex/0109026).

[53] http://www-btev.fnal.gov/public/hep/general/proposal/index.shtml

[54] G. Burdman, *Phys. Rev. D.*, **57**, (1998) (hep-ph/9710550).

[55] See *B Decays, revised 2nd Edition* ed. S. Stone, World Scientific, Singapore, (1994).

[56] B. Aubert *et al.*, *Phys. Rev. Lett.* **87**, 091801 (2001), *ibid.* **86**, 2525 (2001), and B. Aubert *et al.*, "A Study of Time-Dependent CP-Violating Asymmetries and Flavor Oscillations in Neutral B Decays at the Upsilon(4S)," (hep-ex/0201020) (2002); K. Abe etal, *Phys. Rev. Lett.* **87**, 091802 (2001).

[57] B. Aubert *et al.* (BABAR), "Study of CP-violating asymmetries in $B^o \to \pi^+\pi^-$, $K^+\pi^-$ decays," (hep-ex/0110062) (2001).

[58] Z. Zhao *et al.*, "Report of Snowmass 2001 Working Group E2: Electron-positron Colliders from the ϕ to the Z," to appear in the proceedings (hep-ex/0201047).

[59] S. Henderson, "M2: Summary -Electron-Positron Circular Colliders," presented at Snowmass 2001, to appear in the proceedings, http://vmsstreamer1.fnal.gov/VMS_Site_02/Lectures/Snowmass2001/720M2Henderson/sld016.htm

[60] DOE/NSF HIGH-ENERGY PHYSICS ADVISORY PANEL SUBPANEL ON LONG RANGE PLANNING FOR U.S. HIGH-ENERGY PHYSICS, available at http://doe-hep.hep.net/.

[61] P. Ball *et al.*, "B decays at the LHC," CERN-TH/2000-101 (hep-ph-0003238).

[62] K. Abe *et al.*, (CDF), *Phys. Rev. Lett.* **75**, 1451 (1995); S. Abachi *et al.*, (D0), *Phys. Rev. Lett.* **74**, 3548 (1995). See also the UA1 measurement C. Albajar *et al.*, *Phys. Lett.* B**186**, 237 (1987); B**213**, 405 (1988); B**256**, 121 (1991).

[63] K. Abe *et al.*, (CDF), *Phys. Rev. Lett.* **76**, 4462 (1996); ibid **77**, 1945 (1996); K. Abe *et al.*, (CDF), *Phys. Rev. D* **57**, 5382 (1998).

[64] T. Junk, "A Review of B Hadron Lifetime Measurements from LEP, the Tevatron and SLC," in Proceedings of the 2nd Int. Conf. on *B Physics and CP Violation*, Univ. of Hawaii, (1997), ed. T. E. Browder *et al.*, World Scientific, Singapore (1998).

[65] K. Abe *et al.*, (CDF), "Observation of B_c Mesons in $p-\overline{p}$ Collisions at $\sqrt{s} = 1.8$ TeV," hep-ex/9804014 (1998).

[66] M. Paulini, "B Lifetimes, Mixing and CP Violation at CDF," Review article to appear in the Int. Journal of Modern Physics A, hep-ex/9903002 (1999).

[67] K. Anikeev *et al.*, "B Physis at the Tevatron: Run II and Beyond, "FERMILAB-PUB-01/197 (hep-ph/0201071) (2001).

[68] "LHCb Technical Proposal," CERN/LHCC 98-4, LHCC/P4 (1998), available at http://lhcb.cern.ch .

[69] See T. Nakada, "LHCb Light status and related issue," at http://lhcb-doc.web.cern.ch/lhcb-doc/progress/progress.htm

[70] We have confirmed with T. Nakada, the LHCb spokesperson, that the yields for this mode as quoted in their Technical Proposal are their current values that we should use in our comparisons. The branching ratio numbers used by LHCb were taken from Table 15.11 on page 157. The number of events were taken from Table 15.12. Since these numbers are quoted as being "tagged," we divided by the 0.40 tagging efficiency given on page 145. The two final states $\rho^+\pi^-$ and $\rho^-\pi^+$ are given separately by LHCb; we added them together. The same procedure was followed for $B_s \to D_s K$.

[71] P. Ball *et al.*, "B Decays at the LHC," CERN-TH/2000-101, hep-ph/0003238.

[72] Although they state a 1% efficiency here, this is only a partial efficiency according to T. Nakada.